4-30-2018

Multipurpose Glider-Quadcopter UAS

Cody Delarosa
Kennesaw State University

Lucas Richards
Kennesaw State University

Ty Hilton
Kennesaw State University

Multipurpose Glider-Quadcopter UAS

Technical Report

Team Name: Down 2 Fly

Cody Delarosa: Technical Expert, Failure Analyst

Lucas Richards: CAD Designer, Simulation Expert, Literature Analyst

Ty Hilton: Project Manager, Financial Officer, Software Coordinator

Advisor: Dr. Adeel Khalid

Submitted: April 30, 2018

Table of Contents

Executive Summary

The goal for this design was to develop a dual stage UAS that will deliver medical supplies to people in need in remote locations. To accomplish this, a quadcopter was designed to release a glider with the payload therein. A scaled down prototype was produced for analysis purposes. A conceptual model was fully designed that is capable of effectively taking off vertically, accelerating to a desired velocity, releasing the glider, and returning back to the initial takeoff location. The glider was designed to be fully controllable in order to accurately reach the desired location. System aerodynamics and quadcopter propulsion were thoroughly studied throughout the design process in order to optimize range. Computational fluid dynamics, finite element analysis, and extensive hand calculations were completed on both component geometries and propulsion systems in order to verify final system effectiveness. It was determined that the range requirement of 10 miles for the entire system could be accomplished with a maximum velocity of 128 mph.

Chapter 1

Introduction

The unmanned aerial system (UAS) designed involves a quadcopter which deploys a glider mid-flight. After being released, the glider delivers the payload to its target destination. Using two separable vehicles provides the opportunity to have a diverse range of specifications for the aircraft. The payload may be a small package of food, medicine, or other essential supplies. The general goal of the aircraft is to deliver the payload effectively and efficiently. To accomplish this, predetermined design requirements were established.

Design component interactions were placed under heavy scrutinization to meet the design requirements. Hand calculations and computer aided simulations were used to assess conceptual models while the prototype was tested physically. The working model developed had lowered design requirements in order for the entire system's functionality to be analyzed without a heavy manufacturing cost.

System Overview

Due to the nature of the design, system components needed to be broken into two separate categories. While going through the design process, the separate aircraft were also designed in this way, however it was important to optimize for entire system performance. Therefore, often times the two aircraft were compared with one other to ensure functionality. Table 1 illustrates the components specific to each aircraft .

Table 1. Component Overview

Quadcopter	Glider
Battery	Battery
Flight Controller	Servo Motors for Control Surfaces (4)
Power Distribution Board	Payload Compartment
Receiver	Syringes Holder
Transmitter (Controller)	Medicine Vials
Propellers (4)	Camera
Brushless Motors (4)	Avionics
Frame	Flight Controller
Electromagnetic Release	Receiver
Electronic Speed Controllers (ESCs)	Transmitter

Objective

The objective is to design a two part quadcopter and glider UAS to deliver a specified payload to a previously determined location. The quadcopter, with the glider attached, will take off vertically from ground level and elevate to a specified altitude. From here it will increase its speed towards the target until it achieves a previously specified velocity. Then, the glider, with the payload inside, will detach from the quadcopter and proceed towards the previously determined location. The quadcopter will recede to the initial takeoff location. The glider will safely perform a crash landing at the targeted location, allowing the payload to be retrieved from within.

Justification

People in need in remote villages of war-torn countries often fall victim to preventable diseases due to a lack of access to vaccinations. Currently, programs like UNICEF are working hard to deliver these vaccines to the remote locations. Often times these workers are forced to trek across miles of mountainous terrain, cross rivers, and even cross battle lines to bring these vaccinations to the people. The quadcopter glider UAS will be able to carry vaccinations faster than workers and will also prevent them from having to put their lives on the line to deliver the vaccines.

Often times, combat can leave military personnel stranded with no way to contact their base. The quadcopter glider UAS could send a phone, as well as other military supply essentials, to aid in keeping personnel in contact with base and prolonging survival until a rescue mission can be conducted. This could also be used in the civilian world by sending a long range phone to people stranded in remote areas. Survival tools, as well as a GPS could be included in the payload to allow the recipient to survive until help can get to them.

Project Background

While brainstorming for a project idea, the team wanted to integrate specific passions for rotary and fixed wing aircraft. Field issues that could benefit from an integrated aircraft were then discussed. The combined advantages of a rotary aircraft (high maneuverability, VTOL, etc) and a fixed wing glider (efficiency, long range, stability, etc) would aid in creating an aircraft capable of completing various missions. Humanitarian aid, military resupply, and civilian search and rescue were all suitable missions for the integrated aircraft design.

Problem Statement

Essential packages must be delivered at a low cost, with high reliability, minimal risk, and reusability by utilizing the concept of aircraft integration.

Chapter 2

Literature Review

[1]Amazon has done a substantial amount of unmanned aircraft system (UAS) research in order to deliver packages for their prime air service. Their basic model for the development of an air traffic system would allow for safe operations of UAS in civil airspace. They specifically optimized for systems operating beyond the line of sight. This system would allow the quadcopters to share information with one another, which would help them avoid obstacles. It would also cut shipping costs drastically for companies. This project may take a while to be operational, but when it is, it will revolutionize package delivery across the U.S. This helped the team conceptualize vehicle integration.

[2]An unmanned aerial glider (UAG) was developed by inventor Aerial Zilberstein to disperse fire fighting substances to put out forest fires. The fuselage is pressurized to maintain structural integrity during flight. The glider is unpowered and also is disposable. This design gave insight to the various applications of a payload carrying UAS glider as well as disposable glider possibilities.

[3]The Quantum Tron is a hybrid UAS which can perform as a quadcopter and also as a propelled glider. It resembles a normal glider except it has propellers on the leading and trailing edge of the wing. The propellers face up during takeoff which gives the aircraft the ability to perform vertical takeoff and landing. After takeoff, the front propellers fold forwards and give the aircraft thrust and the back propellers fold backwards and are unused. The aircraft is also equipped with control surfaces and a vertical and horizontal stabilizer. Even though, this

approach was not chosen for the Multipurpose Glider UAS, it inspired the first stage of the system, where both the glider and quadcopter are connected to one another.

[4]Betaflight Configurator is a drone software programming system that allows users to efficiently program their aircraft to any specific requirements. A process of syncing the flight controller with the receiver, syncing the receiver with the transmitter, programming the flight controller, then programming the electronic speed controllers needed to be completed. "Propwashed" detailed specific instructions on how to set various parameters for the team's quadcopter needs.

[5]Universities from around the country compete in an annual micro-aircraft competition where aircraft are designed on the basis of empty weight and payload. A team out of Worcester Polytechnic Institute chose to base their design on a glider since empty weight is directly proportional to competition scoring. Their report helped verify the team's approach to weight saving, as well as computational methods for aerodynamics.

[6]The EZ Glider Dropper is an instruction manual on how to construct a glider to be deployed from a quadcopter. The quadcopter lifts the glider from a string to a maximum height of 400 feet and then releases it. The glider levels out on its own and slowly descends to the earth. This instructional guide provided ideas for the glider release.

[7] Many components make up a quadcopter that must be accounted for in the design phase. While the battery was by far the largest internal component of the quadcopter, other components also needed to be inside the fuselage. For early design, historical trends for quadcopter component sizing was based on the information laid out on the "Oscar Liang" quadcopter hardware overview. While this served as a good place to start, the team's quadcopter

functionality was to be very different than most, and therefore these changes had to be accounted for in component selection.

[8] For initial glider sizing, payload geometry and weight needed to be outlined. The primary mission, vaccination delivery, required knowledge on size and weight of vaccination utensils. UNICEF mentions relative sizing constraints for vaccination as well as the ranges traveled for the delivery. These allowed glider payload volume to be estimated, as well as verification for glider range.

[9] In order to verify that enough vaccinations could be delivered by the system to make it a practical means of delivery, syringe dimensional analysis needed to be completed. Many syringe manufacturers give this information. However, Restek give specifications regarding outer dimensions that were relevant to this project.

[10] The entire system propulsion is based on the quadcopter thrust capabilities. Due to this, extensive research on motor capabilities was completed. KDE Direct, the motor manufacturer, lists detailed motor specification sheets for each of their products. The quadcopter thrust requirements were known based on previous calculations, and matching motors to these requirements were made possible by utilizing their data sheets and efficiency factors.

[11] PU Foam is a lightweight flexible material which has many applications in the aerospace field, and was selected as the glider wing material. It behaves anisotropically when placed under loads. This property makes it difficult to asses. A study was conducted at Gdańsk University of Technology, Department of Materials Science and Engineering which tested the foam’s mechanical properties at different densities and geometry setups. This data was used in the analysis of the glider’s wings.

Chapter 3

Design Requirements (working model and conceptual model)

For a proof of concept, a working model was designed. A conceptual model capable of carrying out missions for real world applications was designed as well. The requirements for the two were the same, however the numerical specifications were varied. Working model requirements are specified by “a)”. Conceptual model requirements are specified by “b)”.

1. Maximum quadcopter payload shall not be less than:
   a. 2 pounds
   b. 15 pounds
2. Maximum glider payload shall not be less than:
   a. 1 pound
   b. 6 pounds
3. Maximum height quadcopter shall carry glider:
   a. 150 feet
   b. 1000 feet
4. Maximum speed quadcopter shall release glider:
   a. 20 mph
   b. 50 mph
5. Maximum range glider shall travel starting at quadcopter’s maximum height and speed:
   a. 720 feet (2 football fields)
   b. 10 miles
6. Maximum glider weight shall not exceed:
   a. 2 pounds
   b. 9 pounds
7. Maximum quadcopter weight shall not exceed:
   a. 10 pounds
   b. 60 pounds
8. Complete design shall cost no more than:
   a. $300
   b. $4550 ($4450 quadcopter, $100 glider)
9. Characteristic requirements: Detachable system and payload inside glider fuselage.

Minimum Success Criteria

The team hopes to accomplish two primary goals:

1. Design a conceptual model that will not be synthesized in any fashion.
2. Develop a prototype model that will operate in the same way with the same design just at lowered specifications.

Verification Approach

For analysis, the glider and quadcopters main components must be tested without actually synthesising the product in order to reduce manufacturing costs. Thus, simulations with solidworks and hand calculations will be utilized for structural and flow analysis. The aerodynamic components that must be analyzed using flow simulations are the wings, horizontal and vertical stabilizer of the glider, and the propellers of the quadcopters. The structural properties will be computed for the quadcopter and glider parts to make sure both aircrafts can handle the inertial forces exerted on it.

Problem Solving Approach

Initial Design Concepts

In order to determine the best possible design for this multistage aircraft system, a design matrix was utilized. Throughout the brainstorming stage of design, five different designs that could accomplish the system requirements were discussed.

Table 2. Initial Design Matrix

Criteria	Priority Value	Normalized Priority Value	Fabric Wing Glider Drone Hybrid		Eight Rotor Drone Glider Hybrid		Lower Mounted Glider on Drone		Upper Mounted Glider on Drone		Folding Wing Rotor Drone Hybrid	
Efficiency	12.5	0.13	9	1.17	4	.52	6	.78	8	1.04	6	0.78
Manufacturability	12.5	0.13	8	1.04	5	.65	7	.91	7	.91	3	0.39
Low Cost	25.0	0.25	5	1.25	2	.50	6	1.5	6	1.5	2	0.50
Durability	10.0	0.10	2	.20	6	.60	5	.50	7	.70	9	0.90
Range	15.0	0.15	4	.60	4	.60	7	1.05	7	1.05	8	1.20
Stability	10.0	0.10	4	.40	8	.80	9	.90	6	.60	4	0.40
Payload (System)	15.0	0.15	5	.75	9	1.35	6	.90	6	.90	8	1.20
Totals	100.0	1.00		5.41		5.02		6.54		6.7		5.37

The lower and upper mounted glider on quadcopter design concepts were far better than alternative designs. The top two designs were within 3% of each other and therefore could both be acceptable design solutions. Both were analysed further as designing proceeded. See Appendix D for original design sketches.

Preliminary Design Approach

After further analysis, it was determined that the lower mounted glider design would be the best approach. The upper mounted glider design was abandoned due to predicted issues with stability caused by a higher than allowable overall center of gravity. The inherent instability of a top mounted glider would result in near impossible aircraft recovery after maneuvering.

Quadcopter Approach

The fuselage of the quadcopter was designed around the battery size since that was the largest internal component. For ease of assembly, as well as internal component modification, a two part fuselage was desired. Determining a connection type for the two fuselage parts was difficult due to the smaller inner dimensions and plastic material type. It was decided that combining a lip groove style mating face with multiple snap hooks would be the best connection type. With this in mind, it was difficult to design an aerodynamic quadcopter body that could encapsulate all of the internal components while being aesthetically pleasing. After multiple design iterations, this was eventually accomplished.

The quadcopter arms and motor holder were initially designed as separate parts with one end of the arm connecting to the motor holder and the other connecting to the quadcopter body. However, this presented attachment problems because plastic is not easily screwed and glue is not reliable. Thus the motor holder was made to be apart of the quadcopter arm and all four quadcopter arms were designed to connect to one another inside of the fuselage forming a plate to hold the control panel. This integrative design makes the quadcopter structure more reliable because the outer shell of the quadcopter will be holding the arms in place. The arms will attach to one another with snap hooks. Also a slot will be implemented for the arms to slide into the quadcopter body. These slots will be cut in such a way that the rotors are symmetrically placed around the quadcopter fuselage center of gravity. The preliminary quadcopter design is displayed in Appendix E which shows the quadcopter body with all four arms attached.

The quadcopter propeller geometry was chosen based on historical data to maximize thrust for the specific motor. See the extracted data in Appendix I1 (working model) and I2 (conceptual model).

Glider Approach

The fuselage of the glider was modeled using a combination of historical geometric relationships for gliders and calculated lengths based on equations discussed later in the System Design Approach. The primary focus for the fuselage design was minimizing drag and increasing functionality. The mission for the overall project's design was for a payload to be delivered inside of the fuselage. Therefore, a large payload bay with easy access was a necessary feature for the glider fuselage. Similar to the quadcopter, a two part glider fuselage was utilized. The split line for the fuselage was placed so that it intersected the payload bay for easy access upon landing. Once again, a lip groove with snap hook connections was used for connecting the two fuselage components.

Multiple glider release mechanisms were discussed throughout the design process. Initially it was thought that a latching mechanism would be the best route. However, after completing a design matrix, it was found that the use of electromagnets far outweighed all other design alternatives. The decision matrix (Table 3) can be found below. The most important criteria for this facet of the design were low cost and reliability. This solution provides a simple, yet reliable release as well as being extremely effective in terms of speed of release and resistance. Also, it was determined that due to the steep angle the quadcopter must be at to reach the maximum defined speed, a flare maneuver must be performed just before release to achieve a nominal release angle for maximum glider range. This maneuver needs to be performed quickly and as close to release as possible to avoid large amounts of speed reduction.

Table 3: Release Mechanism Design Matrix

Release Mechanism Design Matrix										
Criteria	Priority Value	Normalized Priority Value	track plus single release		double latch release		Wing unfold as quad copter accelerates		Electromagnet	
Stability	10.0	0.10	6	0.6	4	0.4	6	0.6	6	0.6
Low Cost	30.0	0.30	3	0.9	6	1.8	4	1.2	8	2.4
Low Weight	20.0	0.20	4	0.8	6	1.2	2	0.4	8	1.6
Reliability	30.0	0.30	8	2.4	6	1.8	6	1.8	9	2.7
Simplicity	10.0	0.10	3	0.3	6	0.6	4	0.4	10	1
Totals	100.0	1.00		**5**		**5.8**		4.4		8.3

Wing geometry and sizing for the glider primarily came from utilizing a series of equations and historical trend data. These equations and calculations are outlined in System Design Approach. The process began by calculating the lift-to-drag ratio for a glider which is simply the horizontal distance traveled divided by altitude lost. From there, glide ratio, drag, lift, wing loading (W/S), aspect ratio, wing area, wing span, and all other critical wing geometry factors could be calculated. With all of these calculated variables, along with historical trend based estimates such as thickness-to-chord ratio (t/c), taper ratio, and sweep angle, an airfoil could be selected that satisfied all specific lift and drag requirements. The calculated Reyonolds number allowed a specific angle of incidence to be selected for the chosen airfoil.

The horizontal and vertical stabilizers were designed to counterbalance the moment caused by the generated lift of the wing. The horizontal and vertical tail areas were calculated by taking the wing’s area, chord length, and span into account, along with assumed values for the tail volume coefficients and the length between the wing quarter chord and vertical and horizontal tail quarter chords which were assumed to be the same.

The vertical and horizontal tail were tapered with the trailing edge of both surfaces being perpendicular to the fuselage longitudinal axis. This design makes the span, root chord, and tip chord easily computable with the calculated areas and assumed aspect and taper ratios that were acquired from referencing historical data.

The thickness to chord ratio of the horizontal tail was assumed to be the same as the wing and the same airfoil was used for simplification purposes. The thickness to chord ratio of the vertical tail was also assumed to be the same as the wing, however an uncambered airfoil was chosen. Knowing the base dimensions of the empennage allows the wing relative location to the fuselage to be calculated, and also provides the opportunity to conduct flow simulations on the entire aircraft.

System Design Approach

Working Model Approach

Cost was the determining factor of deciding the total thrust the working system will generate. The team conducted motor research and found an adequate design that gave a maximum thrust of 12.88 lbs (3.22 lbs/motor). A load factor of two was chosen to calculate total system weight (6.44 lbs). For supplying power to the motor at maximum thrust output, a battery between 15.4 and 17.4 maximum voltage with 4 cells in series (4S) was chosen. Justification on using this battery was determined from the maximum continuous current (34 Amps for 180 seconds). Using equation 1, where (t) is time in minutes, (I_B) is the battery capacity in *mAh*, (Q_m) is motor quantity, (I_{Mmax}) is maximum continuous current drawn from motor, quadcopter operating time at maximum power was calculated to be 1.41 minutes (84 seconds).

$$t = \frac{I_b * 60}{Q_m * I_{Mmax}} = \frac{3.2\ (amps*hours)*60(\frac{minutes}{hours})}{4*34(amps)} = 1.41(min) \quad \textbf{Equation 1}$$

Motor burnout factor of safety was then calculated using equation 2, where $(t_{I_{Mmax}})$ is time for motor burnout at maximum continuous current.

$$FOS = \frac{t_{I_{Mmax}}}{t} = \frac{180\ (sec)}{84\ (sec)} = 2.14 \quad \textbf{Equation 2}$$

Table 4. Prototype Component Weights

Component	Wt./Item (lbs)	Qty	Total (lbs)
Battery	.67	1	.67
Propellers	.004	4	.016
Motors	.093	4	.37
Housing Frame	0.184	1	0.184
Motor Holder Arms	0.0463	4	0.185
Max Glider/Payload	2	1	2
Total			3.425

The table above allowed quadcopter takeoff weight to be calculated. Maximum thrust from the motors is known to be 12.88 lbs with a load factor of 2. Thus, total takeoff weight needed to be no more than 6.44 lbs. The total weight came out to be 3.425 which gives an actual load factor of 3.76.

<u>Conceptual Model Approach</u>

The mission requirements themselves specified a payload for the conceptual model approach. From that payload, a minimum thrust requirement could be calculated. However, after more refined component design, the best motors for the specific design could be chosen. An iterative process between motor selection, propeller, battery selection, and quadcopter fuselage design allowed the best possible design to be selected in order to maximize performance and minimize cost. Once this was completed, the propeller that satisfied the thrust requirements was chosen. See the extracted data for the conceptual motor in Appendix I2. The iterative process for thrust requirements and quadcopter time aloft at 100% power is seen in Appendix I3. Equation 1 was used to calculate this time. Once again, a minimum load factor of 2 was desired for the quadcopter, therefore the minimum thrust required was calculated by using the equation below:

$$T_{min} = W_{total} * 2 \qquad \textbf{Equation 3}$$

The last estimate for total weight came out to be 30 lb. The conceptual quadcopter fuselage geometry was also based on the battery. However, the battery geometry for the conceptual motor was vastly different than that of the working model. Therefore, the conceptual quadcopter fuselage used a varied scale for each coordinate direction. These scaling factors can be seen in Appendix I4. The selected conceptual motor operates best with a battery whose maximum voltage is between 46.2 and 52.2 V and is a 12 series battery. A 21.5” x 7.3 dual propeller provides the maximum amount of thrust for this motor. The maximum thrust is 25.02 lb/motor, giving a total thrust of 100.08 lb. Therefore, the load factor for the quadcopter is 3.336, exceeding the minimum load factor.

Glider geometry began by estimating overall glider weight with the payload. This was 15 lb. Wing geometry began by estimating a thickness-to-chord ratio (t/c) based on historical trends for highly efficient gliders. It was found that the wing t/c should be between 8 and 10%. Next, lift-to-drag ratio was calculated for the glider using the below equation:

$$\frac{L}{D} = \frac{horizontal\ distance\ traveled}{altitude\ lost} = \frac{52800}{1000} = 52.8 = glide\ ratio \qquad \textbf{Equation 4}$$

This number is consistent with current high efficiency gliders on the market. Glide angle (γ) could then be calculated using the below equation:

$$\gamma = tan^{-1}(D/L) = 1.085° \quad \textbf{Equation 5}$$

Wing aspect ratio was then calculated by using the below equation where a and c are glider/sailplane constants:

$$AR = a(\frac{L}{D})^c = .86(52.8)^{1.3} = 32.98 \quad \textbf{Equation 6}$$

An iterative process was then used to determine the best wingspan (b) for the glider. This was done by calculating a wing loading (W/S) that would be as close to possible to 6, which was a historical estimate for sailplanes/gliders. The spreadsheet used to complete this iterative process can be seen in Appendix J1. S was calculated using the below equation:

$$S = \frac{b^2}{AR} = \frac{8.97^2}{32.97} = 2.44\, ft^2 \quad \textbf{Equation 7}$$

Then wing loading for each option was calculated by simply dividing total weight (15 lb) by surface area of the wing. W/S came out to be 6.15 lb/ft^2. In order to verify the required lift-to-drag ratio, the below equations were used to find the dynamic pressure (q), Lift, Drag, coefficient of lift (C_L), coefficient of drag (C_D), and C_L/C_D:

$$q = (1/2)\rho V^2 = (1/2)(.00231)(73.33)^2 = 6.21\ psf \quad \textbf{Equation 8}$$

$$L = W cos\gamma = 5.9989\ lb \quad \textbf{Equation 9}$$

$$D = W sin\gamma = .1136\ lb \quad \textbf{Equation 10}$$

$$C_L = \frac{L}{qS} = 0.396 \quad \textbf{Equation 11}$$

$$C_D = \frac{D}{qS} = 0.0075 \quad \textbf{Equation 12}$$

$$\frac{C_L}{C_D} = 52.8 \quad \textbf{Equation 13}$$

Taper ratio (**λ**) and sweep angle (Λ) were then estimated and optimized based on historical trends and glider flight. **λ**=0.4 and Λ=0. These were chosen to produce the most lift possible and due to the low gliding speeds, the reduced drag from a swept wing will not produce enough of an advantage to quantify doing this. Chord root, tip, and mean aerodynamic chord were then calculated using the equations below:

$$c_{root} = \frac{2S}{(b(1+\lambda))} = 0.3886\,ft = 4.68"$$ **Equation 14**

$$c_{tip} = \lambda c_{root} = 0.155\,ft = 1.872"$$ **Equation 15**

$$\check{c} = (2/3)c_{root}(1 + \lambda + \lambda^2)/(1 + \lambda) = 3.468"$$ **Equation 16**

In order to select the best airfoil for the specified flight conditions, Reynolds number (Re) was calculated using the below equation:

$$Re = \frac{v\check{c}}{\nu} \approx 140,000$$ **Equation 17**

Using the calculated c_L/c_D, the estimated t/c, and the calculated Re, an airfoil could be selected. After analyzing various airfoils, the NACA 6409 was determined to be the best option based on the previously listed criteria. Linear interpolation was then used to determine maximum c_L/c_D based on Re. The maximum c_L/c_D was found to be 71.8, which satisfies the 58.2 requirement. In order to attain this c_L/c_D, an angle of attack (***α***) of 8 degrees was needed. Therefore, an angle of incidence of 8 degrees was used. Appendix J2 shows the profile, data, and graphs for the NACA 6409 airfoil. Lastly, the glider fuselage length was determined using the following equation:

$$Length = aW_0^{\,c} = .86(15)^{.48} = 3.155\,ft = 37.862"$$ **Equation 18**

The horizontal and vertical tail areas were calculated to be 15.9 in^2 and 19.8 in^2 respectively. These values were computed with the two equations below. The length between the wing and empennage quarter chord (LHT & LVT) was assumed to be 65% of the fuselage which came out to be 24.6 in. The mean wing chord (č **),** wing area (SW) and wing span (bW) were calculated above to be 3.468 inches, 352.6 in^2, and 107.64 inches respectively. The horizontal and vertical tail volume coefficients were assumed to be 0.5 and 0.02 for sailplanes and were acquired from Table 6.4 in *Aircraft Design, A Conceptual Approach (Raymer)*.

$$S_{HT} = \frac{c_{HT} \check{c} S_W}{L_{HT}} = \frac{(0.5)(3.468)(352.6)}{24.6} = 15.9\ in^2$$ **Equation 19**

$$S_{VT} = \frac{c_{VT} b_W S_W}{L_{VT}} = \frac{(0.02)(107.64)(352.6)}{24.6} = 19.8\ in^2$$ **Equation 20**

The aspect and taper ratios for both surfaces were assumed to be 8 and 0.4 respectively for the horizontal tail and 1.75 and 0.5 respectively for the vertical tail. These values were averaged from the range in Table 4.3 from *Aircraft Design, A Conceptual Approach (Raymer)*. With these values and the calculated areas, the span (b), tip chord (Ctip), and root chord (Croot) were computed for both the horizontal and vertical tails by solving the system of equations given below which include the Equation 15 & 16 and a rearrangement of Equation 7 from above. This yielded b, Ctip, and Croot to be 11.3 inches, 0.8 inches, and 2 inches respectively for the horizontal tail. The vertical tail's b, Ctip, and Croot came out to be 5.9 inches, 2.25 inches, and 4.5 inches respectively. The thickness to chord ratio of the wing (9%) was applied for both tail geometries along with the same airfoil NACA 6409 for the horizontal tail. However, for the vertical tail, an uncambered airfoil was selected, NACA 0009.

The ailerons for the glider were calculated using equation 21 below. Where (b_a)is the aileron span, (b) is the wingspan, ($\check{c}_a$) is the mean aileron chord, and (č) is the mean wing chord. The aileron span was estimated to be 4.485 feet or 50% of the wingspan, based on historical data. After having the mean aileron chord, the root chord of the ailerons ($c_{root(a)}$) and the tip chord of the ailerons ($c_{tip(a)}$) can be found using equations 22 and 23 where lambda (λ) is the taper ratio of the ailerons. The same taper ratio as the wing was used in order to maintain a constant percent chord of the ailerons. With ($c_{root(a)}$) and ($c_{tip(a)}$) found, the span was ran parallel with the leading edge. The ailerons span was maintained in between 30% and 80% of the wingspan.

$$\frac{b_a}{b} = \frac{\check{c}_a}{\check{c}} = \frac{4.485\,ft}{8.97\,ft} = \frac{\check{c}_a}{.249\,ft} = \check{c}_a = .1445\,ft \quad \textbf{Equation 21}$$

$$c_{root(a)} = \frac{\check{c}_a * 3(1+\lambda)}{2(1+\lambda+\lambda^2)} = \frac{.1445*3*(1+.4)}{2(1+.4+.4^2)} = .194519\,ft \quad \textbf{Equation 22}$$

$$c_{tip(a)} = \lambda * c_{root(a)} = .0778\,ft \quad \textbf{Equation 23}$$

The elevator and rudder were calculated using historical data on control surface sizing guidelines found in table 6.5 of *Aircraft Design, A Conceptual Approach (Raymer)* for a sailplane. The elevator c_e/c equals 0.43 and rudder c_r/c equals 0.40. The root chord of the elevator is $c_{root(e)}$, $c_{tip(e)}$ is tip chord of the elevator, and the abbreviations with (ht) and (vt) are the horizontal and vertical tail components of the chord.

$$c_{root(e)} = c_{root(ht)} * .43 = 2\ in * .43 = .86\ in \quad \textbf{Equation 24}$$

$$c_{tip(e)} = c_{tip(ht)} * .43 = .344\ in \quad \textbf{Equation 25}$$

$$c_{root(r)} = c_{root(vt)} * .40 = 4.5\ in * .40 = 1.8\ in \quad \textbf{Equation 26}$$

$$c_{tip(r)} = c_{tip(vt)} * .40 = 2.25\ in * .40 = .9\ in \quad \textbf{Equation 27}$$

The elevators and rudder only extends to 90% of the horizontal and vertical tail while keeping the same taper ratio in order to have the same constant percent chord.

Once all of the glider components were designed and sized, the center of gravity (CG) could be found using CAD. With that information, wing location could be found using the following equation:

$$CG = 0.3\check{c} = -\ 14.80''\ from\ fuselage\ nose \quad \textbf{Equation 28}$$

With the entire glider designed, including the payload bay, payload design could be completed. While this is a multipurpose UAS, the most likely use for the design is immunization deliveries to remote locations across harsh landscapes. With that in mind, a common large syringe size of 5 cubic centimeters was chosen for the payload. With this size, a total of 17 immunizations could be carried inside of the glider fuselage with the required 85 cubic centimeters of liquid medicine also included. See Appendix J3 for reference.

Avionics

A basic wiring diagram was formulated to fully understand how the system will be connected in both the working and conceptual design. The power supply (battery) is wired to a power distribution board, which distributes the power to each of the electronic speed controls (ESC) and the relay for the electromagnet. The ESC controls the current going to the motor allowing the user to control the rpms of each individual motor. These ESC also has a battery eliminator circuit (BEC) built into it, which will drop the voltage down to 3.3-5 volts in order to power the flight controller and the receiver. The Flight controller directly connects to the ESC allowing control over the motors. The receiver transmits the input from the user, giving control over the entire system. For the release mechanism, a relay is wired up normally closed (n/c) allowing the power to constantly be flown to the electromagnet. Once a signal is sent from the transmitter, the relay will open the circuit, cutting off power, and allowing the electromagnet to shut off and drop the payload.

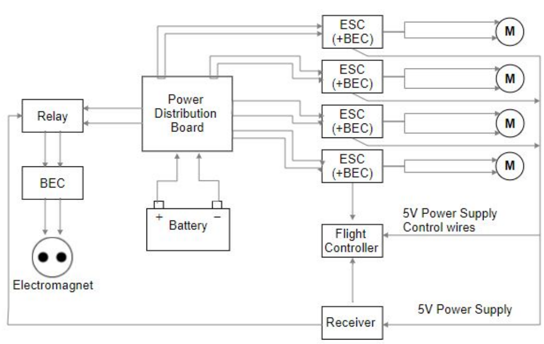

WIRING DIAGRAM Quad Copter	DRAWN BY Down 2 Fly	CHECKED	DATE 3/16/2018	SCALE	SHEET NO. 1

Figure 1. Quadcopter Avionics Schematic

Schedule

Tasks	Week 1 (1/8-1/13)	Week 2 (1/14-1/20)	Week 3 (1/21-1/27)	Week 4 (1/28-2/3)	Week 5 (2/4-2/10)	Week 6 (2/11-2/17)	Week 7 (2/18-2/24)	Week 8 (2/25-3/3)	Week 9 (3/4-3/10)	Week 10 (3/11-3/17)	Week 11 (3/18-3/24)	Week 12 (3/25-3/31)	Week 13 (4/1-4/7)	Week 14 (4/8-4/14)	Week 15 (4/15-4/21)	Week 16 (4/22-4/30)
Team Project/Title	■															
IDR		■	■													
PDR			■	■	■	■	■									
IPR							■	■	■	■	■					
CDR											■	■	■	■		
FDR														■	■	■
Youtube Video/Presentation														■	■	■
quadcopter Research/Analysis/Assembly				■	■	■	■	■								
Glider Research/Analysis/Assembly								■	■	■	■	■				
Complete Design/Testing													■	■	■	

Figure 2: Gantt Chart

Mission Profile

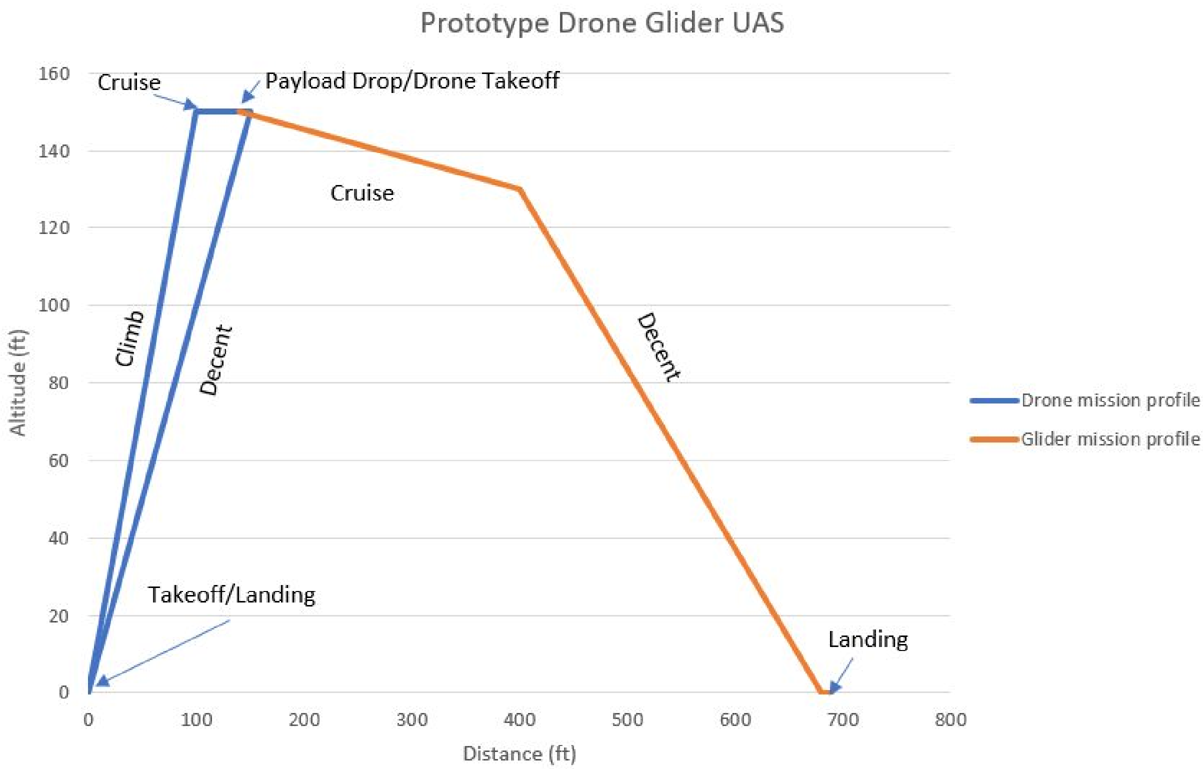

Figure 3. Mission Profile

Project Management

Phase 1

In order to complete phase 1 of the project, which involves the development of the quadcopter, the design was sectioned into four different but dependent categories as listed below.

1. Thrust Capabilities: This will focus on what propels the quadcopter, including battery voltage matched with motor selection, and blade design to maximize lift. This is where the design begins as it governs quadcopter maximum payload.

2. Structural Design: Once acceptable motors are selected, the following can be done: body sizing, aerodynamic design, design for components (arms, fuselage, glider holder, etc), and material selection.
3. Avionics: This will be done concurrently with the structural design to make sure all of the electronic hardware can fit inside quadcopter and not exceed weight limits. This includes matching the flight controller with the battery voltage and acquiring a transmitter and receiver.
4. Glider Base Design: Glider sizing and preliminary design will focus on developing the quadcopter release mechanism and how the glider will be attached to the quadcopter. In order to achieve this, the glider's conceptual size will be determined. It is important to note that in phase 1, the working model design will not go past initial sizing calculations.

These sections are not chronological because the first steps rely on the last. Figure 4 shows the relationship of all four steps. As shown below, the quadcopter design will be evaluated after the glider base design in order for the vehicles to be compatible.

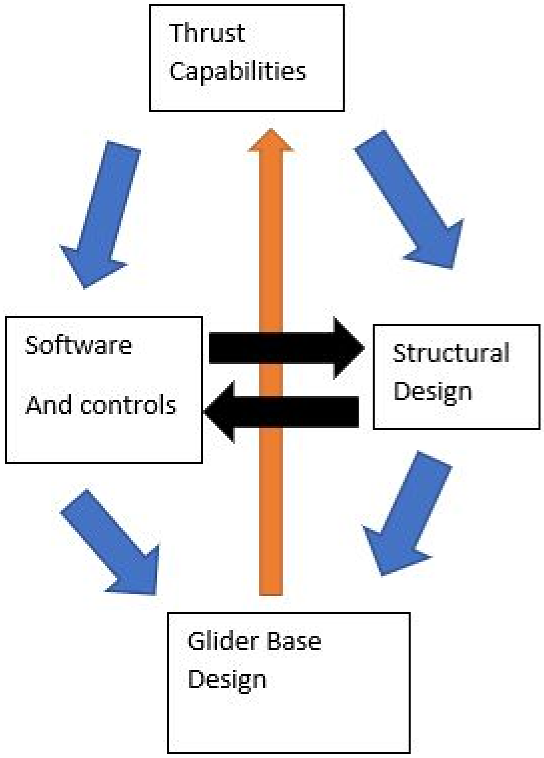

Figure 4. Quadcopter Design Flow Chart

Phase 2

The second phase is comprised of the conceptual model design, integration of both independent vehicles, glider design finalization, and iterating the design based on CAE and hand calculated analysis. The four stages below provide further detail.

1. Conceptual Model Design: The initial sizing for the quadcopter and glider will be conducted. The same procedure for the working model quadcopter will be used.
2. Dual System Integration: Where the release mechanism will be placed relative to both vehicles must be determined, along with the release approach and angle. The quadcopter will fly at an angle, so the structural integrity of the glider's wings will have to be evaluated.

3. Glider Design Finalization: This includes defining tail geometry configuration (T-tail, H-tail, ect.), and designing the control surfaces. The avionics components of the aircraft will also be selected.
4. Structural and Aerodynamic Analysis: Flow and static simulations will be conducted on the quadcopter working and conceptual design, and the glider conceptual design. This will determine what geometries need to be changed based on structural failure or glider instability. This stage will finalize the design and is essentially the encompaes the critical design phase.

Member Responsibilities

Everyone contributed to various design aspects. Ty contributed to design as well as analyzed finances for the design. Lucas contributed to design as well as analyzed relevant literature and technical report information . Cody contributed to design as well as helped with sizing calculations based on technical data.

Available Resources

- SolidWorks & Matlab
- 3D printing
- Textbooks
- Dr. Adeel Khalid

Budget

Working

Working model: $300

Table 5. Quadcopter Working Model Budget

Part	cost (USD)	Component Names
4 Motors	106.55	KDE2306XF-2550 Brushless Motor
Battery	54.99	Venom 15C 4S 3200mAh 14.8V LiPo Drone Battery
Electromagnet	9.34	Grove Electromagnet
3D Printing	30.00	
Propeller	7.99	Quanum Carbon Fiber Propeller 6x4.5 (CW/CCW)
PDB/ESC (+BEC)/Flight Controller combo	94.99	HOBBYWING CRotor MicroCube
Flight Receiver	Donated	Reused
Total Cost	303.86	
Remaining budget:	-3.86	

Conceptual model

$4550 ($4500 for quadcopter, $50 for glider)

Table 6. Quadcopter Conceptual Model Budget

Part	cost (USD)	
4 Motors	792	KDE5215XF-220 Brushless Motor
Battery	540	LiPo 8000 12S 44.4v Dual Core Battery Pack
Power Distribution Board	4.70	Quadcopter Drone Multicopter Power Distribution Board Battery ESC Connection
Electromagnet	22	Uxcell Electromagnet Solenoid
Camera	80	Spy Tec Mobius Action Camera 1080P HD Mini Sports Cam Wide Angle Edition C2 Len
Propeller	293.9	KDE-CF215-DP 21.5" X 7.3, DUAL-EDITION SERIES (CW/CCW PAIR)
ESC (+BEC)	80	Turnigy Brushless ESC 85A w/ 5A SBEC
Flight Controller	169	DJI Naza-M V2 Flight Controller Newest Version 2.0 with GPS All-in-one Design
Transmitter/Receiver	229	Scherrer UHF Tx700 PRO Long Range Transmitter
3D Printing of the Frame	991	ProtoLab
Total Cost	3201.60	
Remaining budget:	1297.40	

Chapter 4

Results

Hand Calculations

Quadcopter Arm Structural Analysis

The conceptual quadcopter arms experience bending stress from the upwards 33.36 N of thrust generated by the motors in hover. The maximum moment results at the point where the arm meets the body. The arm thickens at the root, however for the calculations of the maximum bending stress, the diameter will be treated constant as its smallest dimension. The outer diameter of the arm is 16 mm and its total length is 337 mm. The filleted rectangular cut inside the arm was treated as a circular cut with an equivalent diameter of 10.932 mm. Therefore the maximum bending stress can be calculated by first finding the second moment of inertia and the maximum bending moment.

$$I = \frac{\pi}{32}(0.016^4 - 0.010832^4) = 5.032 * 10^{-9}\ m^4$$ **Equation 29**

$$M = 33.36 \ * 0.337 = 11.24\ N * M$$ **Equation 30**

$$\sigma_{max} = \frac{MC}{I} = \frac{11.24*0.008}{5.032*10^{-9}} = 17.87\ MPa$$ **Equation 31**

High Density Polyethylene has a ultimate tensile strength of 22.1 MPa which gives a minimum factor of safety of 1.24 for the conceptual quadcopter arm..

Finite Element Analysis

Glider Wing Structural Analysis

In order to verify structural integrity of the conceptual glider's wing, FEA was ran on the rigid polyurethane foam. solidworks did not have material properties for this material on hand

and therefore material properties had to be found. The eleventh literature review in this report mentions the study the team found to extrapolate these material properties. The modulus of elasticity was found from the stress-strain curve in the study. The material's poisson's ratio was found in a data table also in the study. The ultimate strength was found by dividing the maximum force at rupture by the cross sectional area of the test specimen. All of this data was then input into solidworks. All stresses found were lower than the extrapolated ultimate strength of the material. For these graphs see Appendix M. For the FEA screenshots, see Appendix K.

Computational Fluid Dynamics

The quadcopter housing drag was determined using two design iterations after scaling. As shown in Appendix L1, the chosen fuselage, which utilized varied scaling, produced less drag and weighed substantially less.

To ensure the glider wing and fuselage were getting ideal pressure and velocity plots at the specified initial velocity, preliminary CFD was done. The results were nominal as shown in Appendix L2.

Horizontal Velocity Verification

An important aspect of the design was the ability to achieve a specified system horizontal velocity to ensure the glider could reach the required range. The best pitch angle was found by understanding that the rear two propellers would spin at a higher rpm than the front two in order to achieve horizontal flight. The back two could produce 50.04 pounds of lift vertically. The front two were selected to fly at the next highest efficiency which would produce 40.88 pounds of lift together. Knowing the total system weight, trigonometry could be used to find the ideal pitch angle for maximum horizontal velocity while achieving vertical balance. It was found to be 19.27°.

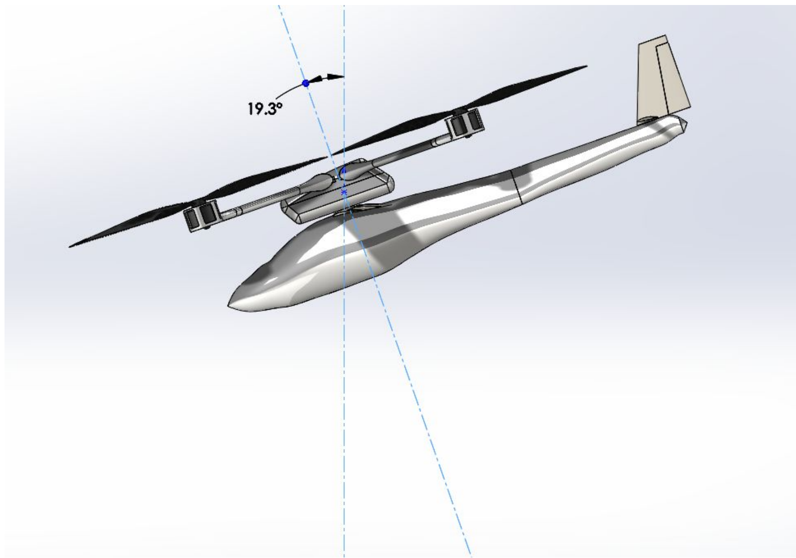

Figure 5. Pitched UAS

The total system was then set to operate at this angle for CFD flow simulations. By varying the freestream velocities, and converging the data at the critical velocity (50 mph), a drag coefficient of 0.522 was found for the entire system at this pitch using equation 32.

$$C_D = \frac{F_D}{.5 * \rho * V^2 * A_{projected}}$$ **Equation 32**

Next the total possible horizontal thrust force at this pitch needed to be found through CFD on the propellers. Simulations were run at both rpms used in calculating pitch angle. The total converged horizontal thrust force was found to be 22.6 pounds. This number was found by using the following equation.

$$T_{horizontal} = 2 * F_{rear\ prop} + 2 * F_{front\ prop}$$ **Equation 33**

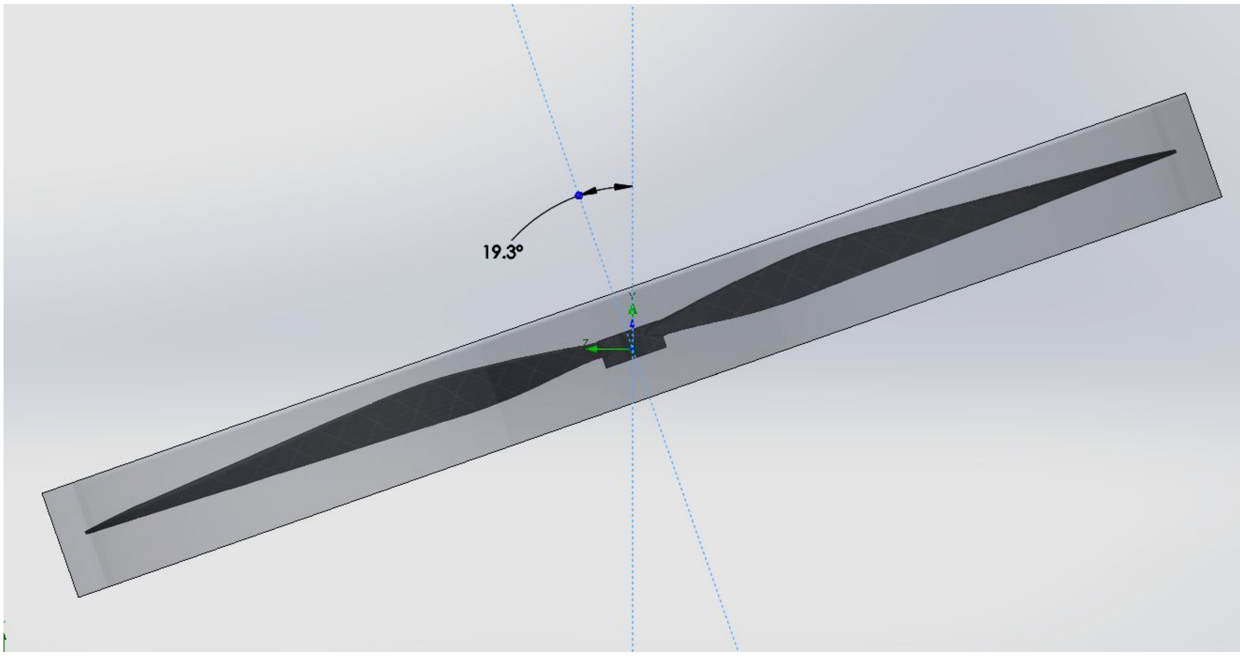

Figure 6. Pitched Propeller

The maximum velocity could then be calculated by utilizing the following equation where drag force is equal to maximum horizontal thrust force for maximum velocity.

$$V_{max} = \sqrt{\frac{T_{horizontal}}{C_D * .5 * \rho * A_{projected}}} = 187.85\ fps = 128\ mph \qquad \textbf{Equation 34}$$

For maximum range optimization, the best constant velocity needed to be found. From the motor data sheet (Appendix I2), amperage ratings for different rpms could be found. By calculating the time in air based on motor amps and battery capacity, total time aloft was known. Then by knowing the maximum velocity from CFD and the time the battery could supply power at that constant velocity, distance flown could be found by multiplying velocity and time. Now, time at different amperages were known, as well as maximum total distance traveled. Velocity for each time could then be found by dividing distance by time. An equation for velocity vs time was then found. Various times were then input into the equation to find the constant velocity at each time point. Final distance traveled was then found by multiplying the velocity and time together. After this the best constant cruising velocity for range optimization could then be found.

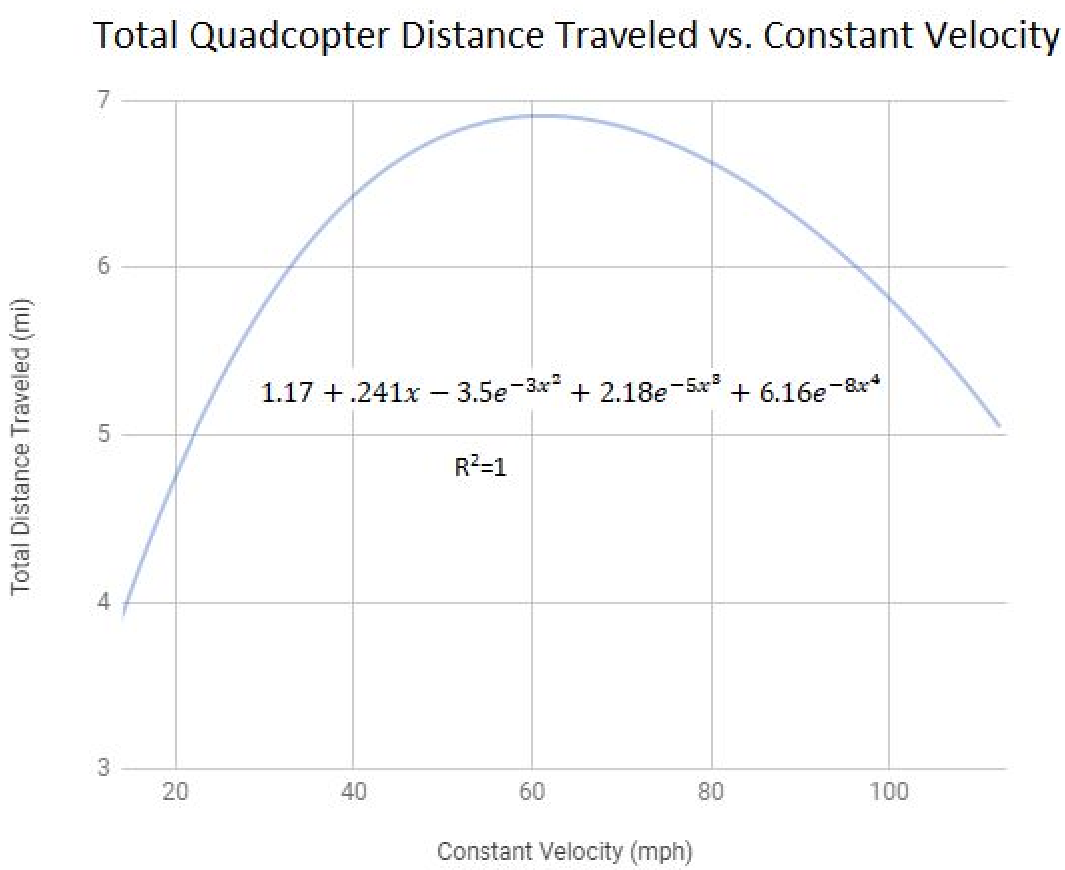

Figure 7. Total Quadcopter Distance vs. Constant Velocity

From this graph, the velocity for maximum range was found to be 62.4 mph. A power curve based solely on horizontal power and velocity was then generated in order to find the most efficient cruise velocity for battery life optimization. The horizontal power available line was found by multiplying the total horizontal thrust force (22.6 pounds) and various velocities together. In order to convert all data to horsepower (hp), the power value was divided by 550. Next, the power required equation could be generated based on CFD data from drag flow simulations. The drag forces from the flow simulations were multiplied by the corresponding velocity values and divided by 550. These curves were than laid over one another to generate the horizontal power curve.

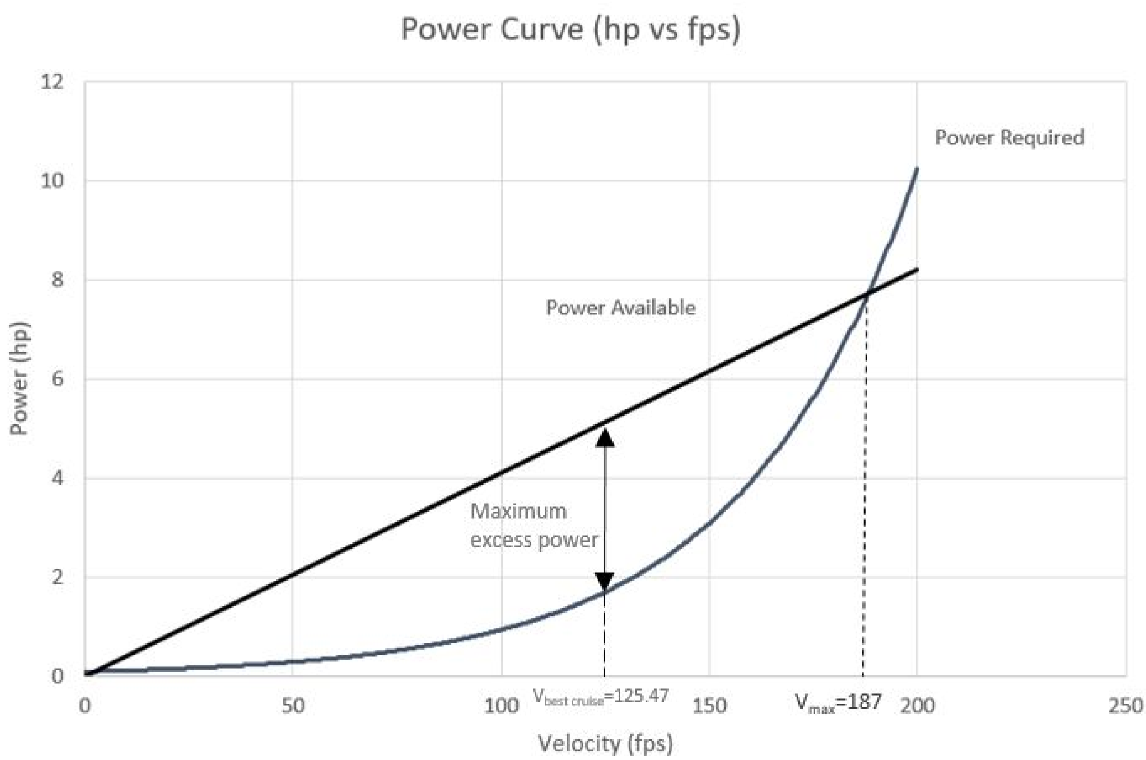

Figure 8. Horizontal Power Curve

The maximum velocity and most efficient cruise velocity was found by utilizing the following techniques.

$$V_{max} \Rightarrow set\ P_a(x) = P_r(x)\ and\ solve\ for\ x \qquad \textbf{Equation 35}$$

$$V_{max} = 187\,fps = 128\ mph$$

$$V_{best\ cruise} \Rightarrow set\ \tfrac{d}{dx}(P_a - P_r) = 0\ and\ solve\ for\ x \qquad \textbf{Equation 36}$$

$$V_{best\ cruise} = 125.47\,fps = 85.5\ mph$$

For all images and numerical data associated with horizontal velocity, reference Appendix N.

Prototype

The working model was constructed with the 3D printed PLA frame, the selected battery, motors, propellers, flight controller, power distribution board, receiver, and controller. See figure in Appendix O, which shows the components laid out. All of the components were correctly sized and worked together, however the 3D printed frame had defects that were not anticipated. First, the arms did not correctly fit with the fuselage as designed. The snap hooks were too small for the printer to synthesis properly and were barely on. The bottom of the fuselage did not fit with the top part of the fuselage properly. The lip grooves were too large which was another printer error. All of these issues were addressed with physical altercations that worked. However, in the end the quadcopter would not lift far off of the ground because the frame was vibrating too much and it was unstable. This unstable movement ultimately snapped one of the motor holders. This was also partially due to the removal of material around the motor in order to make the motors fit. In hindsight, it would have been in the teams best interest to 3D print from a more reliable source. Future prototypes developed will have more secure structures that properly fit to one another with screws or by utilizing a single frame structure. Appendix O displays pictures of the quadcopter before assembly and after. Due to the unforeseen issues, a prefabricated frame was used in order to provide a system proof of concept. This model is shown in Appendix O.

Chapter 5

Conclusion

The two primary goals established for this project were ultimately met with a few alterations. A conceptual model was designed which theoretically satisfies the design requirements. The conceptual quadcopter designed has a maximum speed of 128 mph which is significantly greater than the 50 mph goal. This maximum velocity was acquired through CFD analysis that took into account the propeller's constant thrust of each motor, the pitch of the system, and the system's drag coefficient. The best cruise velocity, 85.5 mph, was also determined to be greater than the 50 mph goal. Also, the quadcopter motor arms experienced a bending stress of 17.87 Mpa which resulted in a factor of safety of 1.24 when compared with the ultimate tensile strength of PE High Density which is 22.1 MPa. The glider wings structural integrity was also verified with Finite Element Analysis (FEA).

Future Recommendations

For the expansion of this project, multiple alterations should be considered for design improvement. The structural and aerodynamic aspects of the frame should be separate. This will help reduce the vibrational effects while keeping the frame optimized for high velocities. The structural frame component should be one solid piece, and if 3D printed, make sure it will be high quality and extremely fine.

Secondly, a more in depth analysis should be conducted on the conceptual model. This should branch into fields such as vibrations, controls, heat transfer, and more in depth material science. This will give insight to any other miscellaneous issues with the design.

References

Brandt, J. B., & Selig, M. S. (n.d.). *Propeller performance Data at Low Reynolds Numbers*(Rep.).

Grove Electromagnet. (n.d.). Retrieved from https://www.robotshop.com/en/grove-electromagnet.html?gclid=CjwKCAjwypjVBRANEiwAJAxlInj2OOlrYCCaaXVXvGydq4ABGsKAZ4uWVPIeLkLD8-vUgynItQ_YrRoCEqcQAvD_BwE

How to Choose Flight Controller for Quadcopter. (2018, April 02). Retrieved from https://oscarliang.com/best-flight-controller-quad-hex-copter/

In photos: How vaccines reach the most remote places on earth. (n.d.). Retrieved from https://www.unicef.org.au/blog/unicef-in-action/april-2017/photos-vaccines-reach-most-remote-places-earth

LiPo 8000 12S 44.4v Dual Core Battery Pack. (n.d.). Retrieved from https://www.maxamps.com/lipo-8000-12s-44-4v-dual-core-battery-pack

Part 7: The Equations for Speed. (2018, April 16). Retrieved from https://quadstardrones.com/the-equations-for-speed/

Quanum Carbon Fiber Propeller 6x4.5 (CW/CCW) (2pcs). (n.d.). Retrieved from https://hobbyking.com/en_us/quanum-carbon-fiber-propeller-6x4-5-cw-ccw-2pcs.html?countrycode=US&gclid=CjwKCAjw-bLVBRBMEiwAmKSB8_n83-m7qcsE_KGxY3xbhy-5fMrlbUw6P-Y_22RSEIFsoNR731DuEBoCeUcQAvD_BwE&gclsrc=aw.ds

Raymer, D. P. (2012). *Aircraft design: A conceptual approach*. Reston, VA: American Institute of Aeronautics and Astronautics.

G. (2012, June 28). SOLIDWORKS - Snap Hook and Groove. Retrieved from https://www.youtube.com/watch?v=00Cz8KPGY5Q

G. (2012, June 28). SOLIDWORKS – Lip Groove. Retrieved from https://www.youtube.com/watch?v=kq1jNkvByyo

Spy Tec Mobius Action Camera 1080P HD Mini Sports Cam Wide Angle Edition C2 Lens. (n.d.). Retrieved from https://www.amazon.com/gp/product/B00GT2B4R6/ref=as_at/?imprToken=MosQbGbZzmljC03P08Kuwg&slotNum=3&ie=UTF8&camp=1789&creative=9325&creativeASIN=B00GT2B4R6&linkCode=w61&tag=drone0e0-20&linkId=SX7AOOGAICS4UFF5

Tips for powering your Flight Controller. (2018, January 25). Retrieved from https://blog.dronetrest.com/tips-for-powering-your-flight-controller/

Uxcell Electromagnet Solenoid. (n.d.). Retrieved from https://www.amazon.com/dp/B00JR6NN3Y/ref=asc_df_B00JR6NN3Y5401074/?tag=hyprod-20&creative=395033&creativeASIN=B00JR6NN3Y&linkCode=df0&hvadid=167121312710&hvpos=1o2&hvnetw=g&hvrand=8002127916932280052&hvpone=&hvptwo=&hvqmt=&hvdev=c&hvdvcmdl=&hvlocint=&hvlocphy=9010789&hvtargid=pla-315951638788

Williamson, G. A., McGranahan, B. D., Broughton, B. A., Deters, R. W., Brandt, J. B., & Selig, M. S. (n.d.). *Summary of Low-Speed Airfoil Data*(Rep.).

Literature Review References

[1] Camhi, J. (2017, May 22). Amazon takes critical step toward drone delivery. Retrieved from http://www.businessinsider.com/amazon-takes-critical-step-toward-drone-delivery-2017-5

[2] US20170240276A1 - Unmanned glider system for payload dispersion. (n.d.). Retrieved from https://patents.google.com/patent/US20170240276A1/en

[3] US20170240276A1 - Unmanned glider system for payload dispersion. (n.d.). Retrieved from https://patents.google.com/patent/US20170240276A1/en

[4] Betaflight Configuration Guide. (2018, April 02). Retrieved from https://www.propwashed.com/betaflight-configuration-guide/

[5] Akhtar, Z., Fredette, R., O'Sullivan, P., & Rosado, D. (n.d.). *Design of A Micro-Aircraft Glider*(Rep.).

[6] Instructables. (2017, September 30). Launch a Glider Via Quadcopter! Retrieved from http://www.instructables.com/id/Launch-a-Glider-Via-Quadcopter/

[7] Quadcopter Hardware Overview - Every Component Explained. (2018, April 26). Retrieved from https://oscarliang.com/quadcopter-hardware-overview/

[8] In photos: How vaccines reach the most remote places on earth. (n.d.). Retrieved from https://www.unicef.org.au/blog/unicef-in-action/april-2017/photos-vaccines-reach-most-remote-places-earth

[9] NORM-JECT Plastic Syringe Specifications. (n.d.). Retrieved from http://www.restek.com/norm-ject-specs

[10] Make It Yours. (n.d.). Retrieved from https://www.kdedirect.com/

[11] Witkiewicz, W., & Zielinski, A. (n.d.). *Properties of The Polyurethane (PU) Light Foams*(Rep.).

Appendices

A. Acknowledgements

The team would like to express much appreciation for those who have made this project possible. The team's advisor, mentor, and professor, Dr. Adeel Khalid deserves a lot of credit for contributing to our team's knowledge on the subject and giving us the skills necessary to complete the project and report. The team would also like to thank Dr. Chance McColl for supplying the needed aerodynamics background to be prepared for this course. Lastly, the team would like to thank Daniel P. Raymer for authoring the course textbook, Aircraft Design: A Conceptual Approach, which serves as a brilliant guide for the team to achieve its goals. The team would like to thank McKayla Jacobs for sharing her electrical expertise with the team and for circuitry tips. A special thanks goes out to each of the team members who worked extremely hard and dedicated a lot of time to coordinate and complete this project and report.

B. Contact Information

Cody Delarosa
Phone: 404-934-6526
Email: codydelarosa93@gmail.com

Lucas Richards
Phone: 770-362-9510
Email: Lb243@aol.com

Ty Hilton
Phone: 678-365-9940
Email: tyguy720@gmail.com

C. Reflections

This project proved to be an incredible learning experience. However, sometimes learning is painful. Minor difficulties were encountered during the conceptual design process. However, these challenges were nothing when compared to the issues faced when the working model was fabricated. To save money, a cost effective quadcopter was 3D printed from a third party at fraction of what other companies offered. This seemed like the best route at the time, however the PLA model was very coarse and the parts did not correctly fit together. Another issue faced during the quadcopter assembly, was the circuitry. Soldering the wires proved to be extremely difficult. The team luckily received professional help which expedited the process significantly. Lastly, when the quadcopter was finally put together, the vibration from the motors combined with the faulty frame assembly, made the UAS too unstable and uncontrollable. Moving forward, the team plans on improving the working model design. If a new model was to be 3D printed, the CAD parts would be altered to be screwed in rather than using snap hooks. Also, more room would be added to the fuselage and more structural support in general.

D. Preliminary hand generated sketches

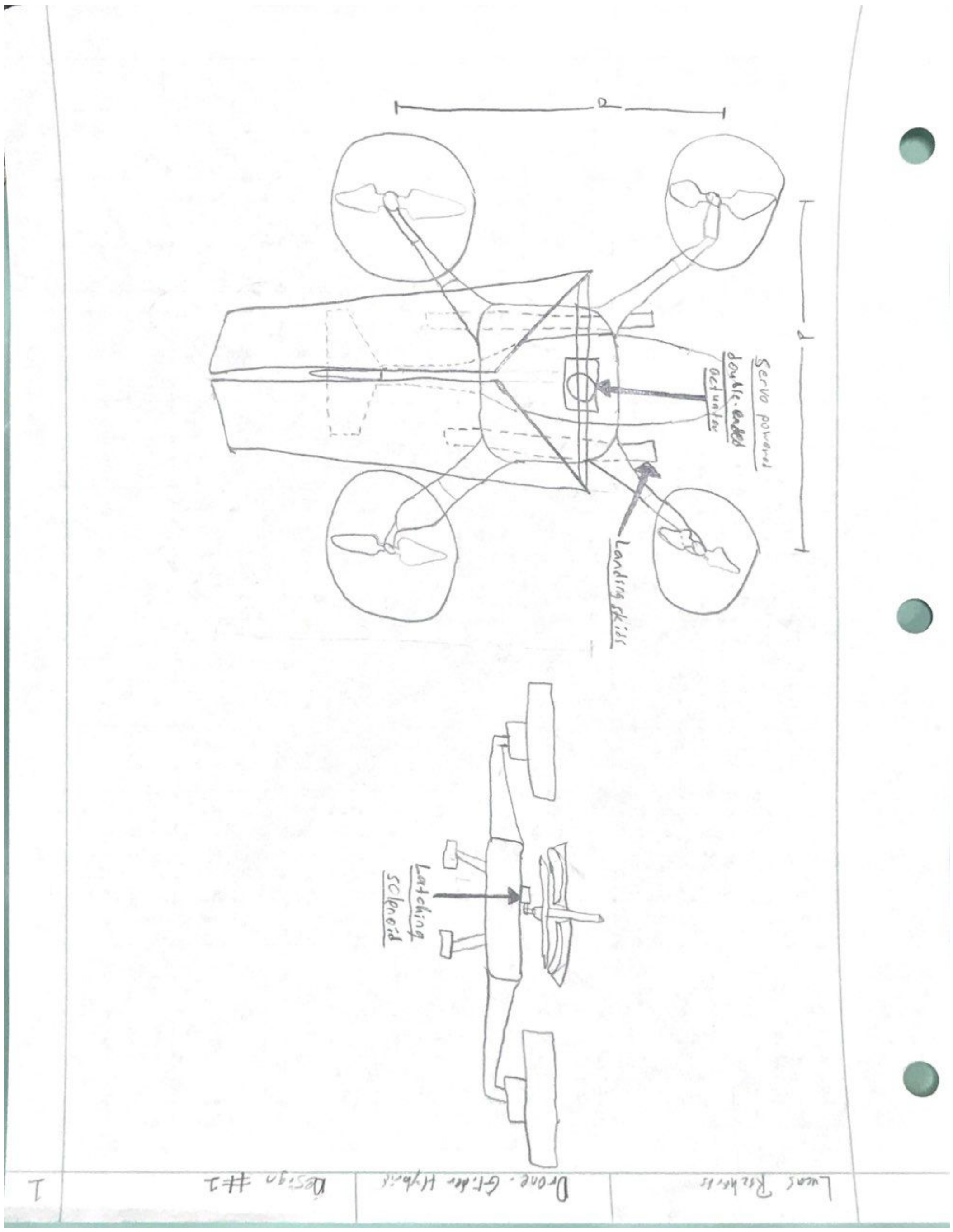

Figure 9. Preliminary Sketch 1

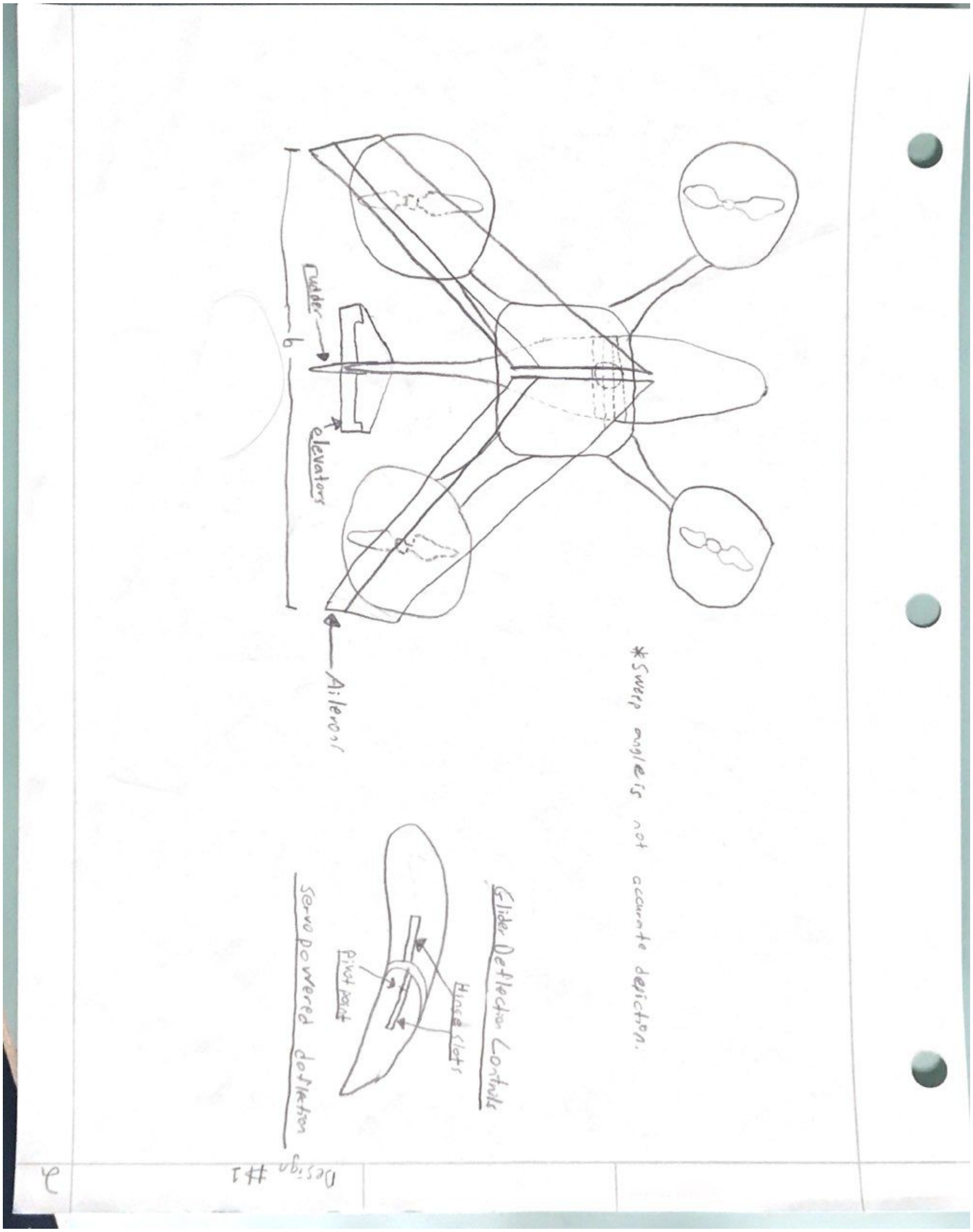

Figure 10. Preliminary Sketch 2

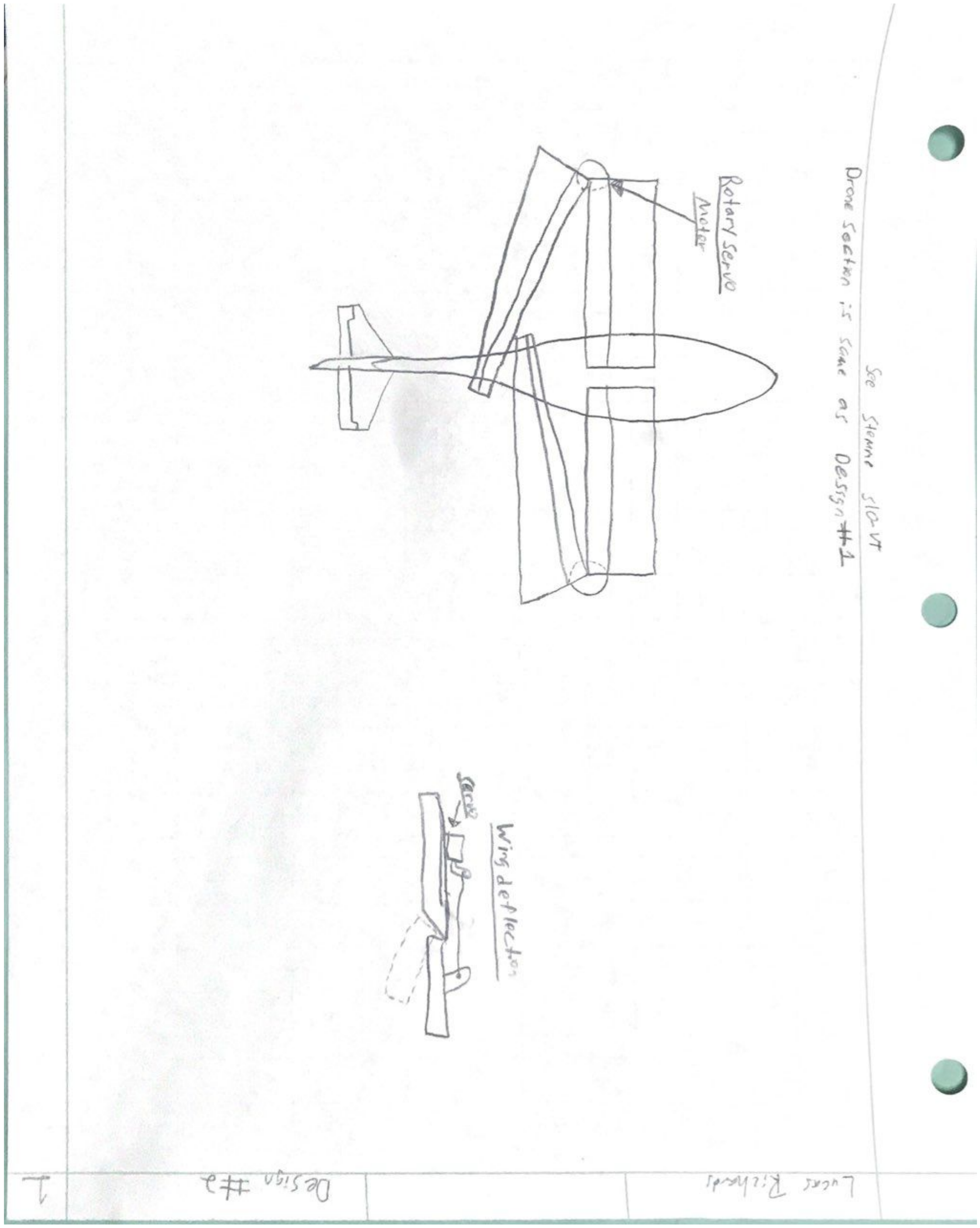

Figure 11. Preliminary Sketch 3

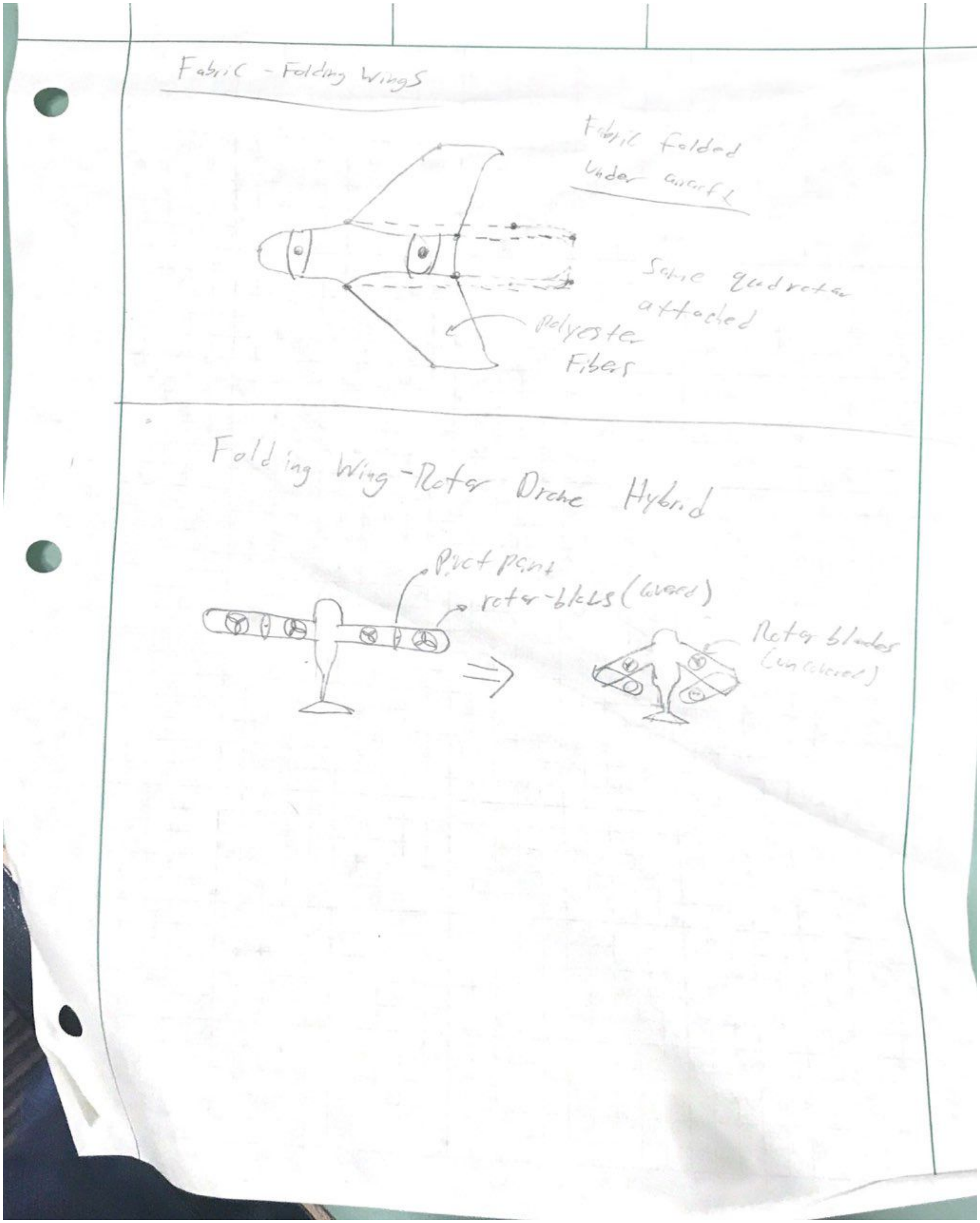

Figure 12. Preliminary Sketch 4

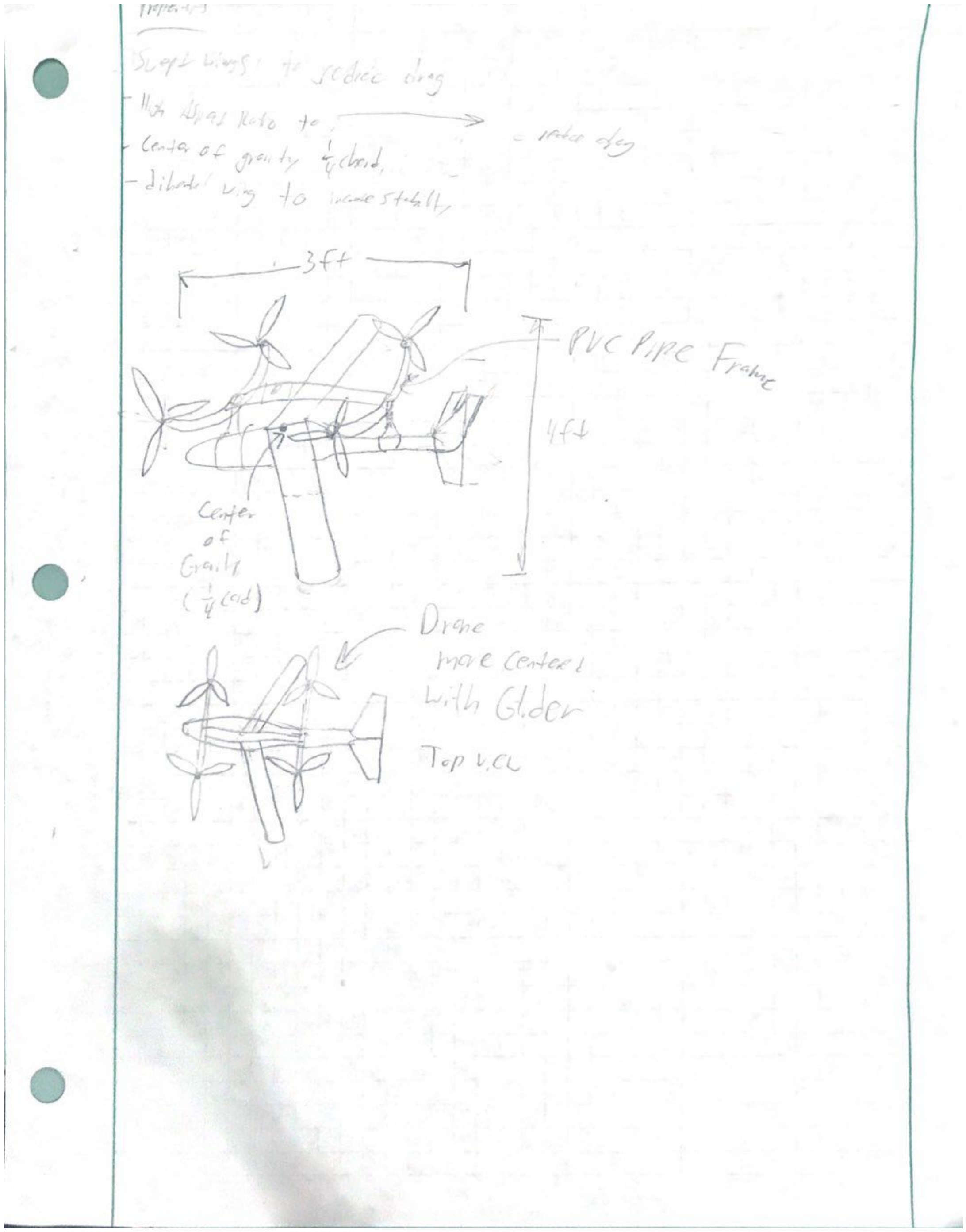

Figure 13. Preliminary Sketch 5

E. Preliminary Design

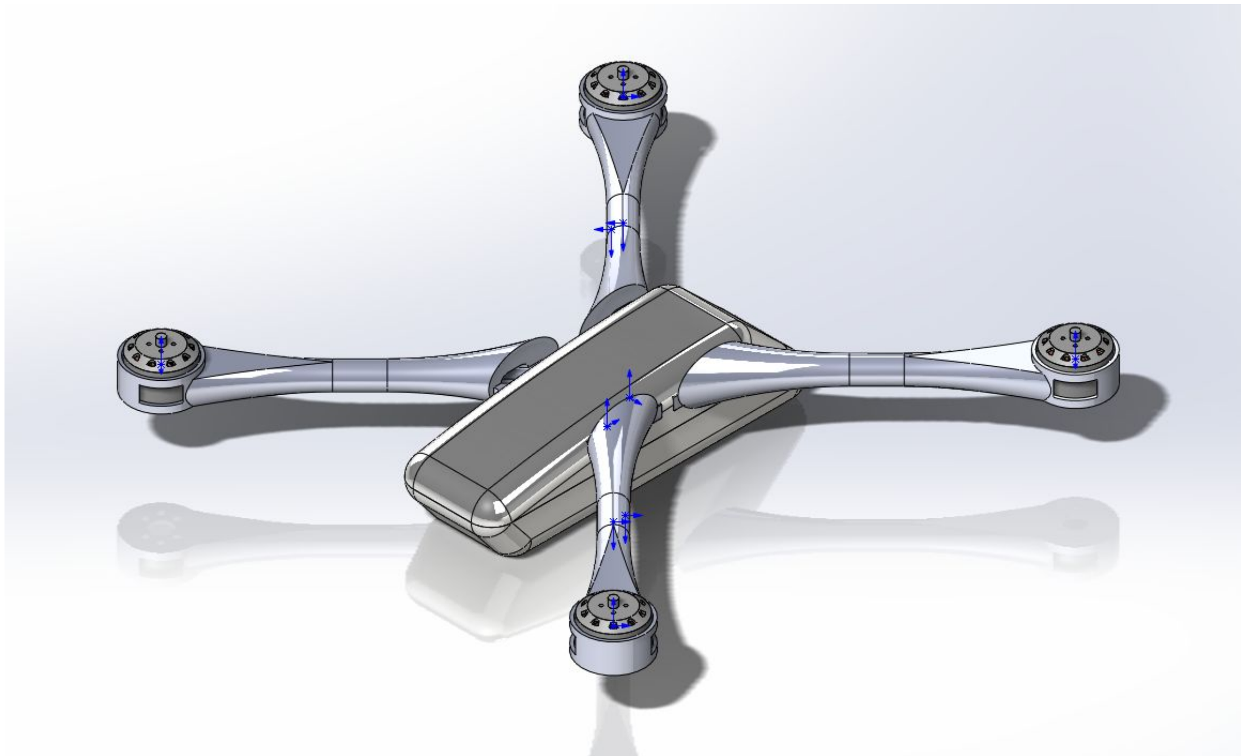

Figure 14. Preliminary Working Design Isometric

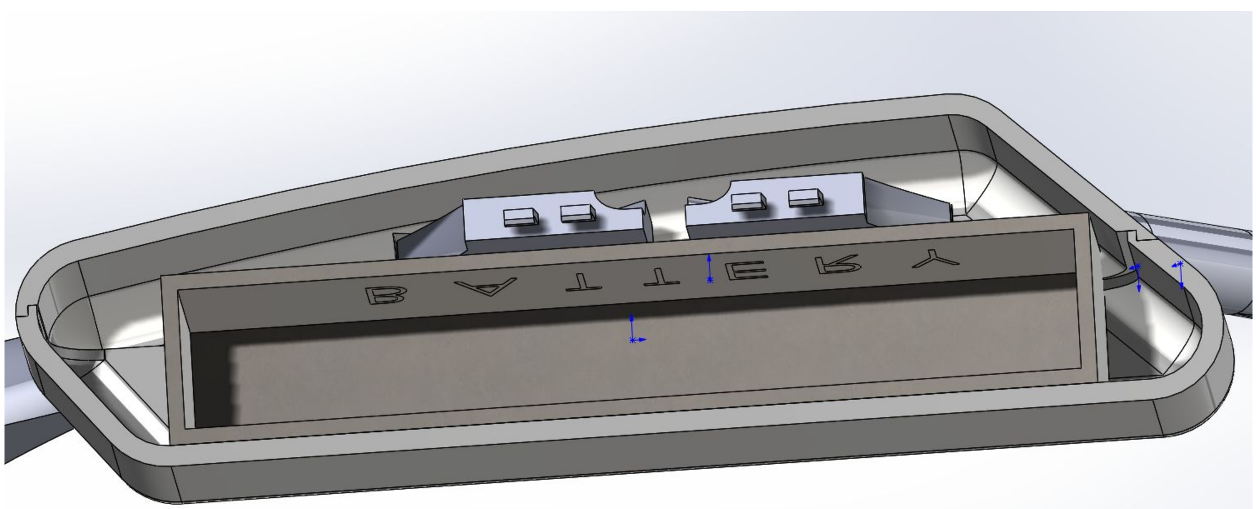

Figure 15. Internal arm connection with battery

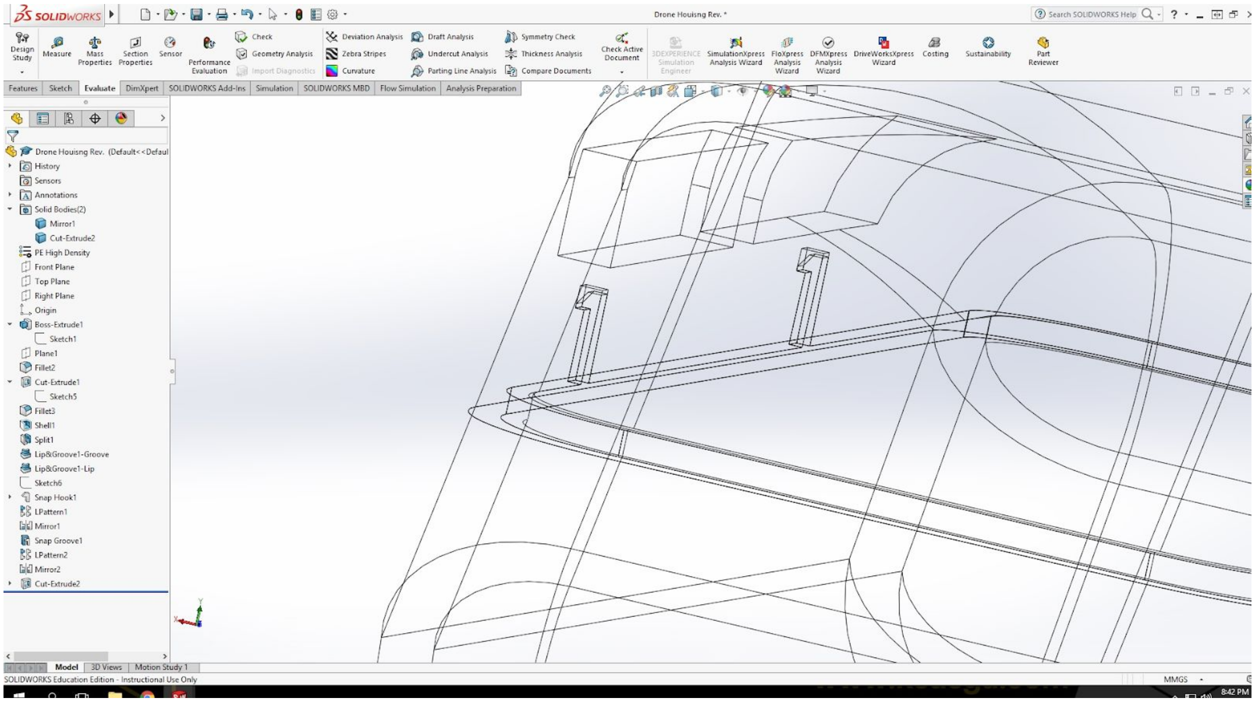

Figure 16. Snap connections for the body of the quadcopter

F. List of Figures

List of Figures

G. List of Tables

List of Tables

H. List of Equations

List of Equations

I. Quadcopter Data

I1: Working Motor Data Sheet

Table 7. Working Motor Data Sheet

MOTOR VERSION	VOLTAGE LiHV [V]	PROPELLER SIZE	THROTTLE RANGE	AMPERAGE [A] (LOWER IS BETTER)	POWER INPUT [W] (LOWER IS BETTER)	POWER INPUT [hp]	THRUST OUTPUT [g] (HIGHER IS BETTER)	THRUST OUTPUT [N]	THRUST OUTPUT [lb]	RPM [rev/min] (HIGHER IS BETTER)	EFFICIENCY [g/W] (HIGHER IS BETTER)	EFFICIENCY [lb/hp]
	15.4V (4S) 17.4V MAX	5" x 3.0HQ	25.0%	2.2	33	0.04	130	1.27	0.29	13980	3.94	6.48
			37.5%	3.2	49	0.07	180	1.77	0.40	16260	3.67	6.04
			50.0%	5.0	77	0.10	280	2.75	0.62	20640	3.64	5.98
			62.5%	7.1	109	0.15	390	3.82	0.86	24240	3.58	5.88
			75.0%	9.1	140	0.19	470	4.61	1.04	26600	3.36	5.52
			87.5%	12.0	184	0.25	600	5.88	1.32	29880	3.26	5.36
			100.0%	15.0	231	0.31	740	7.26	1.63	30920	3.20	5.27
		5" x 4.0HQ	25.0%	2.5	38	0.05	140	1.37	0.31	12480	3.68	6.06
			37.5%	4.0	61	0.08	220	2.16	0.49	15120	3.61	5.93
			50.0%	6.2	95	0.13	330	3.24	0.73	18680	3.47	5.71
			62.5%	9.2	141	0.19	450	4.41	0.99	21900	3.19	5.25
			75.0%	12.2	187	0.25	580	5.69	1.28	24480	3.10	5.10
			87.5%	17.3	266	0.36	750	7.35	1.65	27500	2.82	4.64
			100.0%	21.9	337	0.45	920	9.02	2.03	28440	2.73	4.49
		5" x 4.0 x 3HQ	25.0%	2.8	43	0.06	170	1.67	0.37	11280	3.95	6.50
			37.5%	4.6	70	0.09	250	2.45	0.55	14000	3.57	5.87
			50.0%	7.5	115	0.15	390	3.82	0.86	16600	3.39	5.58
			62.5%	11.4	175	0.23	540	5.30	1.19	19460	3.09	5.07
			75.0%	15.5	238	0.32	670	6.57	1.48	22280	2.82	4.63
			87.5%	22.1	340	0.46	870	8.53	1.92	24460	2.56	4.21
			100.0%	29.1	448	0.60	1110	10.89	2.45	26300	2.48	4.07
		5" x 4.5BNHQ	25.0%	2.9	44	0.06	170	1.67	0.37	10680	3.86	6.35
			37.5%	4.9	75	0.10	270	2.65	0.60	13440	3.60	5.92
			50.0%	8.1	124	0.17	390	3.82	0.86	16320	3.15	5.17
			62.5%	12.4	190	0.25	540	5.30	1.19	19200	2.84	4.67
			75.0%	18.0	277	0.37	700	6.86	1.54	21980	2.53	4.15
			87.5%	26.0	400	0.54	910	8.92	2.01	24840	2.28	3.74
			100.0%	33.1	509	0.68	1110	10.89	2.45	26700	2.18	3.59
		6" x 3.0HQ	25.0%	2.4	36	0.05	170	1.67	0.37	12480	4.72	7.76
			37.5%	3.8	58	0.08	250	2.45	0.55	14900	4.31	7.09
			50.0%	6.1	93	0.12	390	3.82	0.86	18600	4.19	6.89
			62.5%	8.9	137	0.18	540	5.30	1.19	21720	3.94	6.48
			75.0%	12.1	186	0.25	680	6.67	1.50	24420	3.66	6.01
			87.5%	17.3	266	0.36	900	8.83	1.98	27720	3.38	5.56
			100.0%	22.4	344	0.46	1110	10.89	2.45	30380	3.23	5.30
		6" x 4.5HQ	25.0%	3.1	47	0.06	210	2.06	0.46	9900	4.47	7.35
			37.5%	5.5	84	0.11	350	3.43	0.77	12500	4.17	6.85
			50.0%	9.3	143	0.19	530	5.20	1.17	15360	3.71	6.09
			62.5%	14.2	218	0.29	710	6.96	1.57	18060	3.26	5.35
			75.0%	20.7	318	0.43	920	9.02	2.03	20460	2.89	4.76
			87.5%	30.0	462	0.62	1200	11.77	2.65	23160	2.60	4.27
			100.0%	38.6	594	0.80	1460	14.32	3.22	25100	2.46	4.04

I2: Conceptual Motor Data Sheet

Table 8. Conceptual Motor Data Sheet

MOTOR VERSION	VOLTAGE LiHV [V]	PROPELLER SIZE	THROTTLE RANGE	AMPERAGE [A] (LOWER IS BETTER)	POWER INPUT [W] (LOWER IS BETTER)	POWER INPUT [hp]	THRUST OUTPUT [g] (HIGHER IS BETTER)	THRUST OUTPUT [N]	THRUST OUTPUT [lb]	RPM [rev/min] (HIGHER IS BETTER)	EFFICIENCY [g/W] (HIGHER IS BETTER)	EFFICIENCY [lb/h
KDE5215XF-220 (220Kv, HE) DEXF-UAS55HVC S.R. ENABLED	46.2V (12S) 52.2V MAX	15.5" x 5.3 KDE-CF155-DP DUAL-BLADE	25.0%	1.3	60	0.08	620	6.08	1.37	3180	10.33	16.9
			37.5%	2.1	97	0.13	970	9.51	2.14	4060	10.00	16.4
			50.0%	3.7	170	0.23	1490	14.61	3.28	5040	8.76	14.4
			62.5%	6.1	281	0.38	2170	21.28	4.78	6060	7.72	12.7
			75.0%	9.1	420	0.56	2880	28.24	6.35	7020	6.86	11.2
			87.5%	13.0	600	0.80	3760	36.87	8.29	7960	6.27	10.3
			100.0%	17.4	803	1.08	4850	47.56	10.69	8880	6.04	9.93
		15.5" x 5.3 KDE-CF155-TP TRIPLE-BLADE	25.0%	1.5	69	0.09	680	6.67	1.50	3040	9.86	16.2
			37.5%	2.6	120	0.16	1130	11.08	2.49	3920	9.42	15.4
			50.0%	4.4	203	0.27	1740	17.06	3.84	4840	8.57	14.0
			62.5%	7.6	351	0.47	2590	25.40	5.71	5840	7.38	12.1
			75.0%	11.6	535	0.72	3510	34.42	7.74	6800	6.56	10.7
			87.5%	16.6	766	1.03	4490	44.03	9.90	7680	5.86	9.64
			100.0%	21.9	1011	1.36	5680	55.70	12.52	8580	5.62	9.24
		18.5" x 6.3 KDE-CF185-DP DUAL-BLADE	25.0%	1.7	78	0.10	920	9.02	2.03	2940	11.79	19.3
			37.5%	3.1	143	0.19	1550	15.20	3.42	3720	10.84	17.8
			50.0%	5.6	258	0.35	2350	23.05	5.18	4680	9.11	14.9
			62.5%	10.0	462	0.62	3560	34.91	7.85	5640	7.71	12.6
			75.0%	15.1	697	0.93	4740	46.48	10.45	6540	6.80	11.1
			87.5%	21.2	979	1.31	6030	59.13	13.29	7320	6.16	10.1
			100.0%	28.7	1325	1.78	7660	75.12	16.89	8180	5.78	9.50
		18.5" x 6.3 KDE-CF185-TP TRIPLE-BLADE	25.0%	1.9	87	0.12	1050	10.30	2.31	2760	12.07	19.8
			37.5%	3.9	180	0.24	1810	17.75	3.99	3600	10.06	16.5
			50.0%	7.2	332	0.45	2840	27.85	6.26	4480	8.55	14.0
			62.5%	13.0	600	0.80	4250	41.68	9.37	5440	7.08	11.6
			75.0%	19.2	887	1.19	5590	54.82	12.32	6240	6.30	10.3
			87.5%	27.8	1284	1.72	7110	69.73	15.67	7000	5.54	9.10
			100.0%	36.7	1695	2.27	8800	86.30	19.40	7680	5.19	8.54
		21.5" x 7.3 KDE-CF215-DP DUAL-BLADE	25.0%	2.3	106	0.14	1330	13.04	2.93	2520	12.55	20.6
			37.5%	5.6	258	0.35	2540	24.91	5.60	3460	9.84	16.1
			50.0%	10.0	462	0.62	3860	37.85	8.51	4260	8.35	13.7
			62.5%	16.8	776	1.04	5480	53.74	12.08	4840	7.06	11.6
			75.0%	26.0	1201	1.61	7250	71.10	15.98	5780	6.04	9.92
			87.5%	39.4	1820	2.44	9270	90.91	20.44	6460	5.09	8.37
			100.0%	51.3	2370	3.18	11350	111.31	25.02	7020	4.79	7.87

I3: Battery and Motor Comparisons

Table 9. Battery and Motor Comparisons

Drone takeoff weight	Glider takeoff weight	Total Takeoff Weight (lb)	Load Factor	Total Thrust (lb)	Thrust (g)	Thrust(g)/motor	Thrust(lb)/motor
60	15	75	2	150	68038.8	17009.7	37.5
45	15	60		120	54431.04	13607.76	30
30	15	45		90	40823.28	10205.82	22.5
15	**15**	**30**		**60**	**27215.52**	**6803.88**	**15**

	Battery capacity(mAh)	Motor Continuous Current (A)	drone flight time at 100% power (min)
A	8000	85	1.411764706
	6500	85	1.147058824
B	22000	85	3.882352941
	11000	62	2.661290323
	8000	**42**	**2.857142857**

I4: Battery Scale Factors

Table 10. Battery Scale Factors

Battery:				
	Conceptual	Working	Δ (mm)	Scale Factor
x	137	42.5	94.5	3.223529412
y	45	25	20	1.8
z	174	130	44	1.338461538

J. Glider Data

J1: Conceptual Wing Data Sheet

Table 11. Conceptual Wing Data Sheet

AR	Vi	gamma	Vv	b	S	W	W/S	rho 1000'	q	height	distance	L/D	L	D	CL	CD	CL/CD	lambda	c root	c tip	MAC (cbar)	Y bar
32.97446	73.33	1.085	1.389	6	1.091754	15	13.73935	0.00231	6.210768	1000	52800	52.8	5.9989	0.1136	0.884711	0.016753	52.807218	0.4	0.259941	0.103976	0.19309935	1.285714
				5.5	0.917376		16.35097								1.052879	0.019938	52.807218		0.238279	0.095311	0.17700773	1.178571
				5	0.758162		19.78467								1.273983	0.024125	52.807218		0.216617	0.086647	0.16091612	1.071428
				6.5	1.281294		11.70690								0.753836	0.014275	52.807218		0.281603	0.112641	0.20919096	1.392857
				10	3.032650		4.946169								0.318495	0.006031	52.807218		0.433235	0.173294	0.32183225	2.142857
				4	0.485224		30.91355								1.990599	0.037695	52.807218		0.173294	0.069317	0.12873290	0.857142
				5.75	1.002669		14.96005								0.963314	0.018242	52.807218		0.249110	0.099644	0.18505354	1.232142
				7	1.485998		10.09422								0.649991	0.012308	52.807218		0.303265	0.121306	0.22528257	1.5
				8	1.940896		7.728389								0.497649	0.009423	52.807218		0.346588	0.138635	0.25746580	1.714285
				7.5	1.705865		8.793189								0.566215	0.010722	52.807218		0.324926	0.129970	0.24137418	1.607142
				8.5	2.191089		6.845908								0.440824	0.008347	52.807218		0.368250	0.147300	0.27355741	1.821428
				8.25	2.064097		7.267098								0.467946	0.008861	52.807218		0.357419	0.142967	0.26551160	1.767857
				9	2.456446		6.106381								0.393204	0.007446	52.807218		0.389912	0.155964	0.28964902	1.928571
				9.25	2.594811		5.780767								0.372237	0.007048	52.807218		0.400743	0.160297	0.29769483	1.982142
				9.125	2.525155		5.940229								0.382505	0.007243	52.807218		0.395327	0.158131	0.29367192	1.955357
				9.0625	2.490682		6.022446								0.387800	0.007343	52.807218		0.392619	0.157047	0.29166047	1.941964
				8.97	**2.440097**		**6.147295**								**0.395839**	**0.007495**	**52.807218**		**0.388612**	**0.155444**	**0.28868352**	**1.922142**
	Final:																					
	b= 8.97 ft=107.64"																					
	c root= 4.68"																					
	c tip= 1.872"																					
	MAC= 3.468"																					

J2: NACA 6409 Data

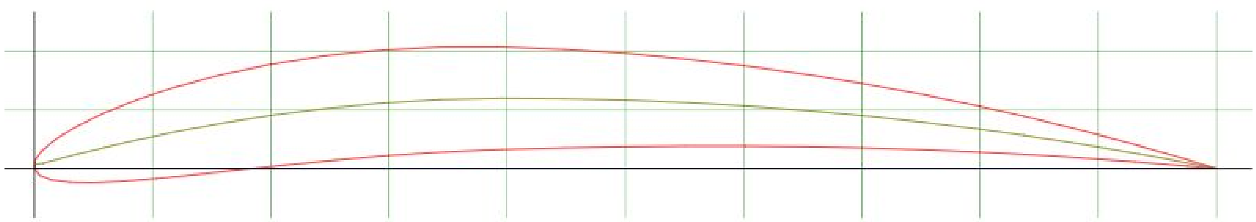

Figure 17. NACA 6409 Airfoil Profile

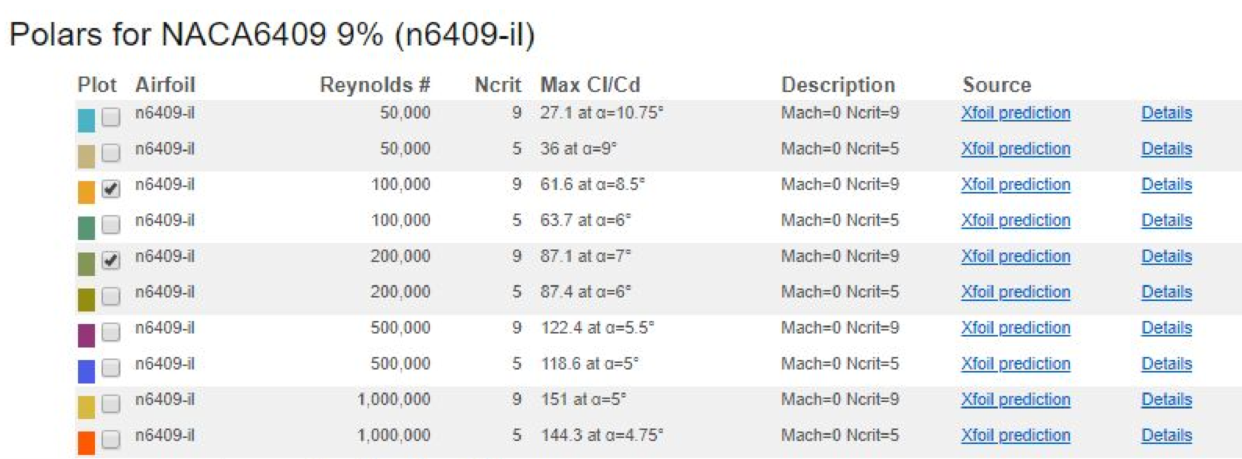

Polars for NACA6409 9% (n6409-il)

Plot	Airfoil	Reynolds #	Ncrit	Max Cl/Cd	Description	Source	
☐	n6409-il	50,000	9	27.1 at α=10.75°	Mach=0 Ncrit=9	Xfoil prediction	Details
☐	n6409-il	50,000	5	36 at α=9°	Mach=0 Ncrit=5	Xfoil prediction	Details
☑	n6409-il	100,000	9	61.6 at α=8.5°	Mach=0 Ncrit=9	Xfoil prediction	Details
☐	n6409-il	100,000	5	63.7 at α=6°	Mach=0 Ncrit=5	Xfoil prediction	Details
☑	n6409-il	200,000	9	87.1 at α=7°	Mach=0 Ncrit=9	Xfoil prediction	Details
☐	n6409-il	200,000	5	87.4 at α=6°	Mach=0 Ncrit=5	Xfoil prediction	Details
☐	n6409-il	500,000	9	122.4 at α=5.5°	Mach=0 Ncrit=9	Xfoil prediction	Details
☐	n6409-il	500,000	5	118.6 at α=5°	Mach=0 Ncrit=5	Xfoil prediction	Details
☐	n6409-il	1,000,000	9	151 at α=5°	Mach=0 Ncrit=9	Xfoil prediction	Details
☐	n6409-il	1,000,000	5	144.3 at α=4.75°	Mach=0 Ncrit=5	Xfoil prediction	Details

Figure 18. Airfoil Data

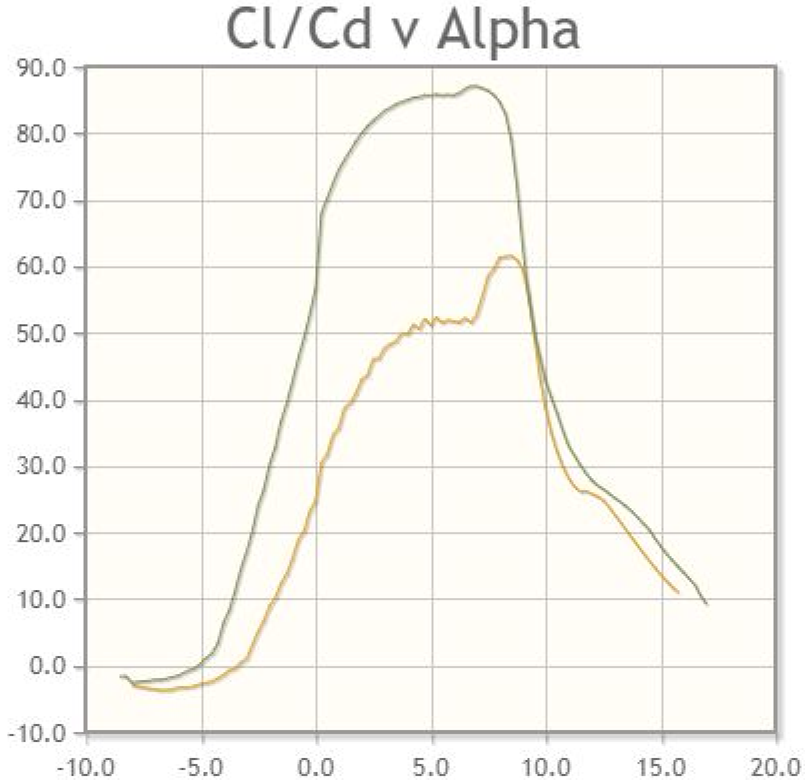

Figure 19. Airfoil Cl/Cd vs Alpha

J3: Conceptual Glider Payload Layout

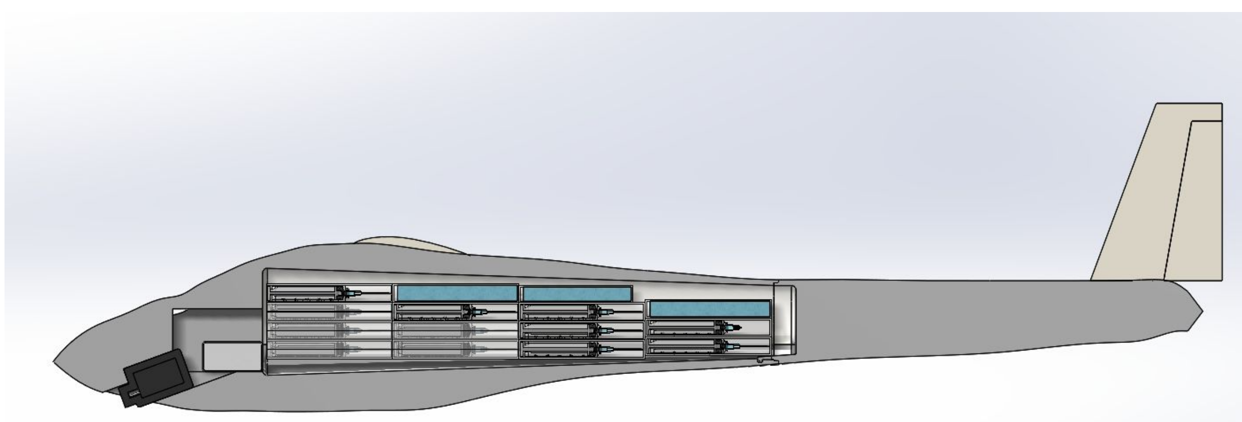

Figure 20. Conceptual Glider Payload Layout

K. FEA

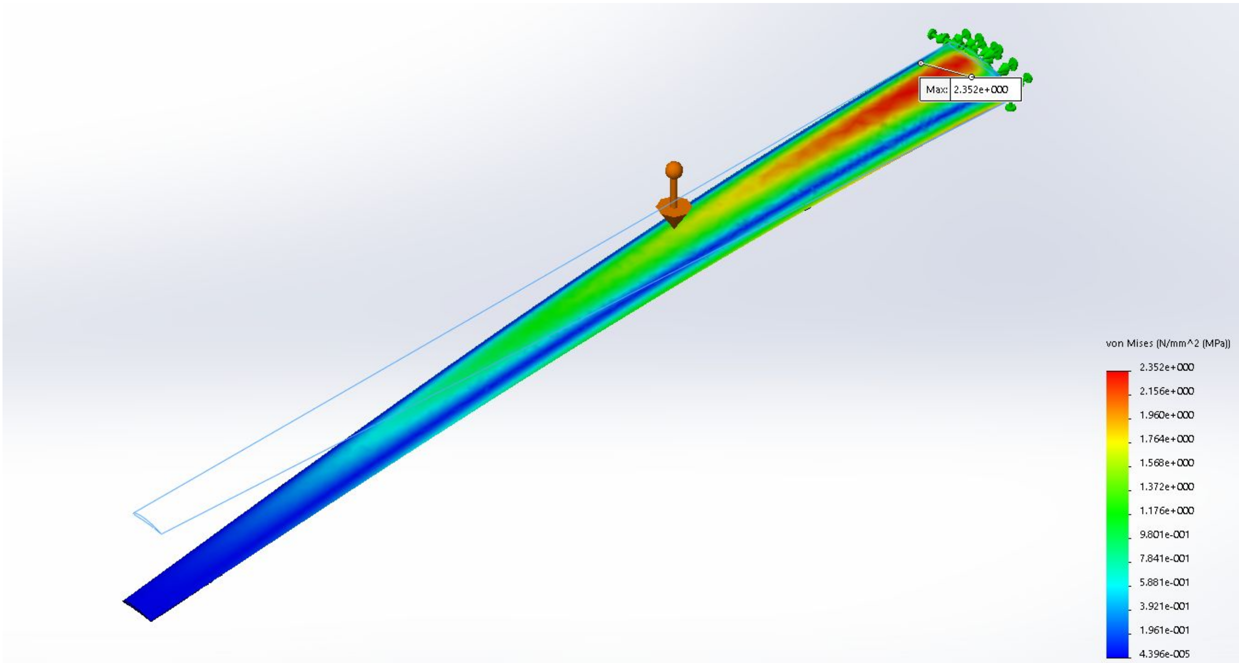

Figure 21. Grounded Glider Wing Stress

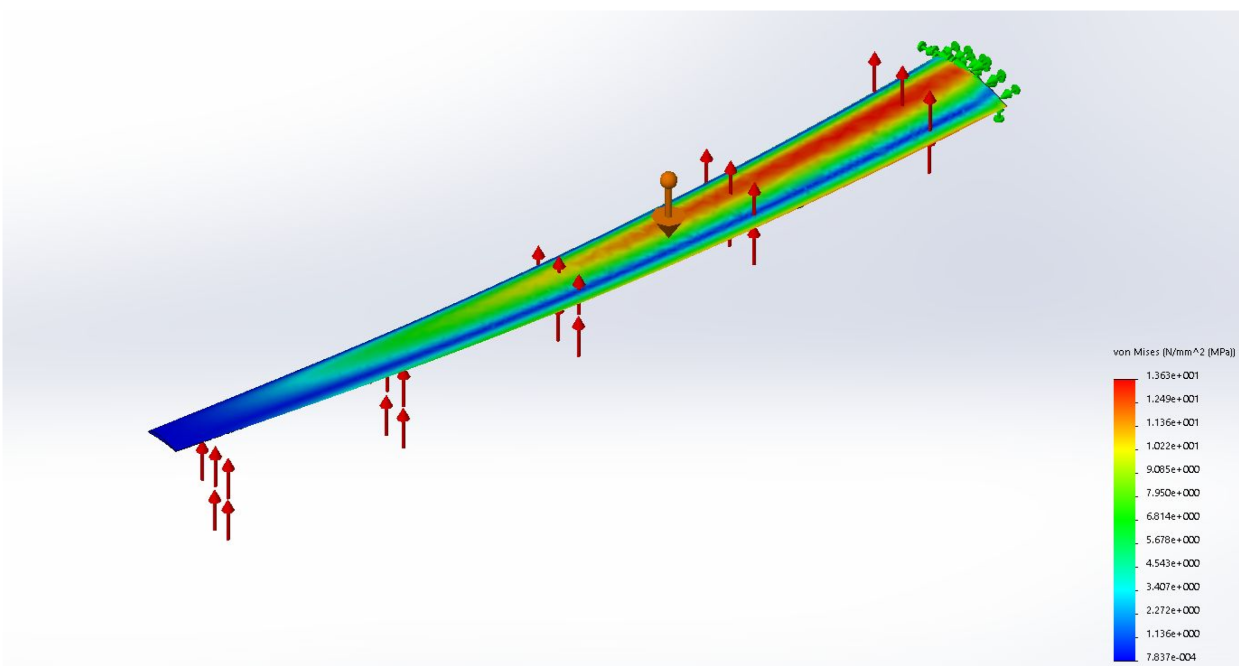

Figure 22. Flying Glider Wing Stress

L. CFD

L1: Quadcopter Fuselage Drag Comparisons

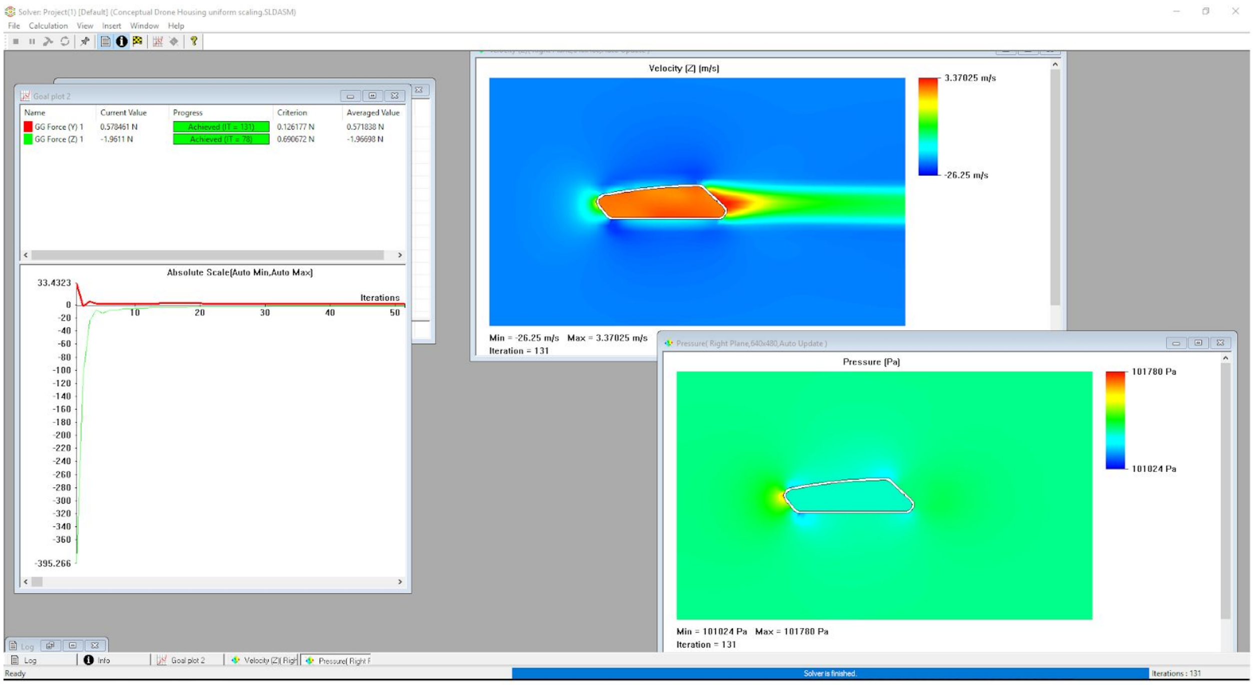

Figure 23. Uniform Scaling Quadcopter Fuselage CFD

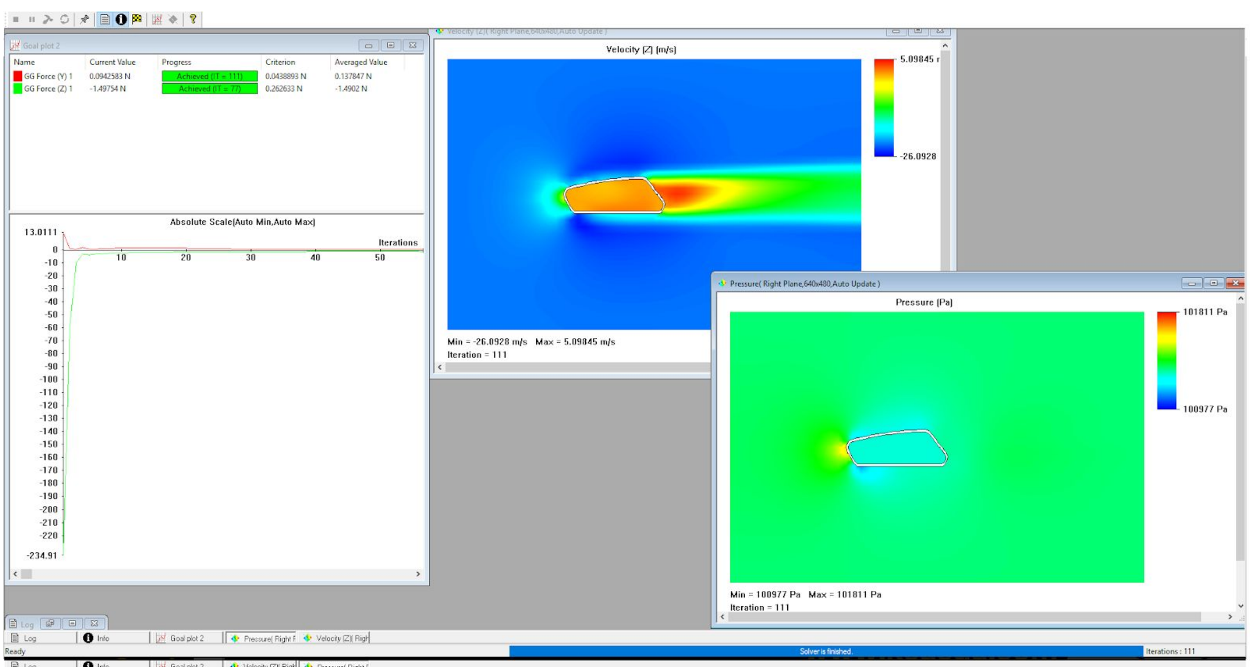

Figure 24. Varied Scaling Quadcopter Fuselage CFD

L2: Glider Wing Contours

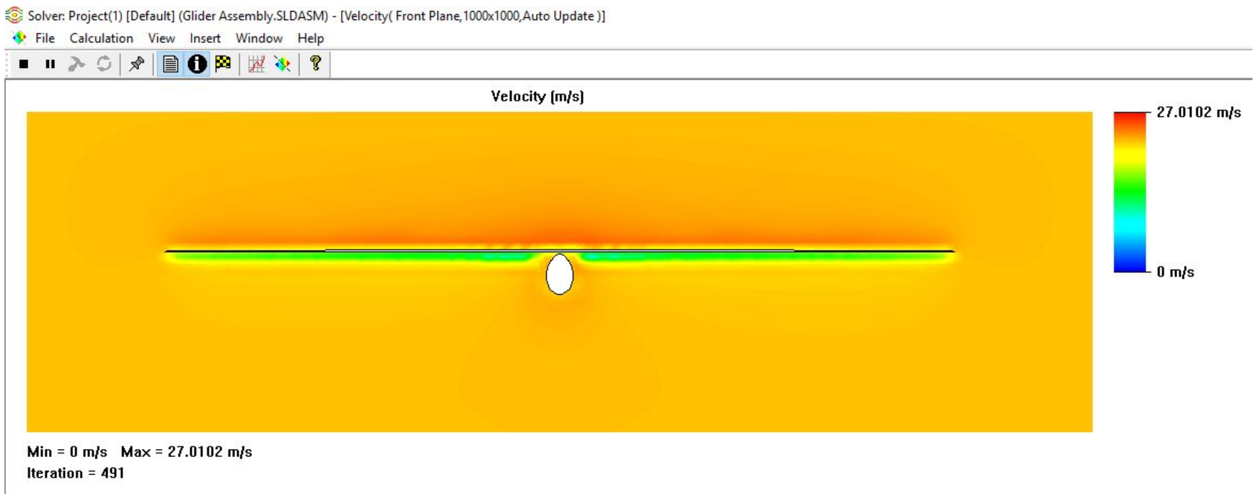

Figure 25. 3D Wing Profile Velocity Contour

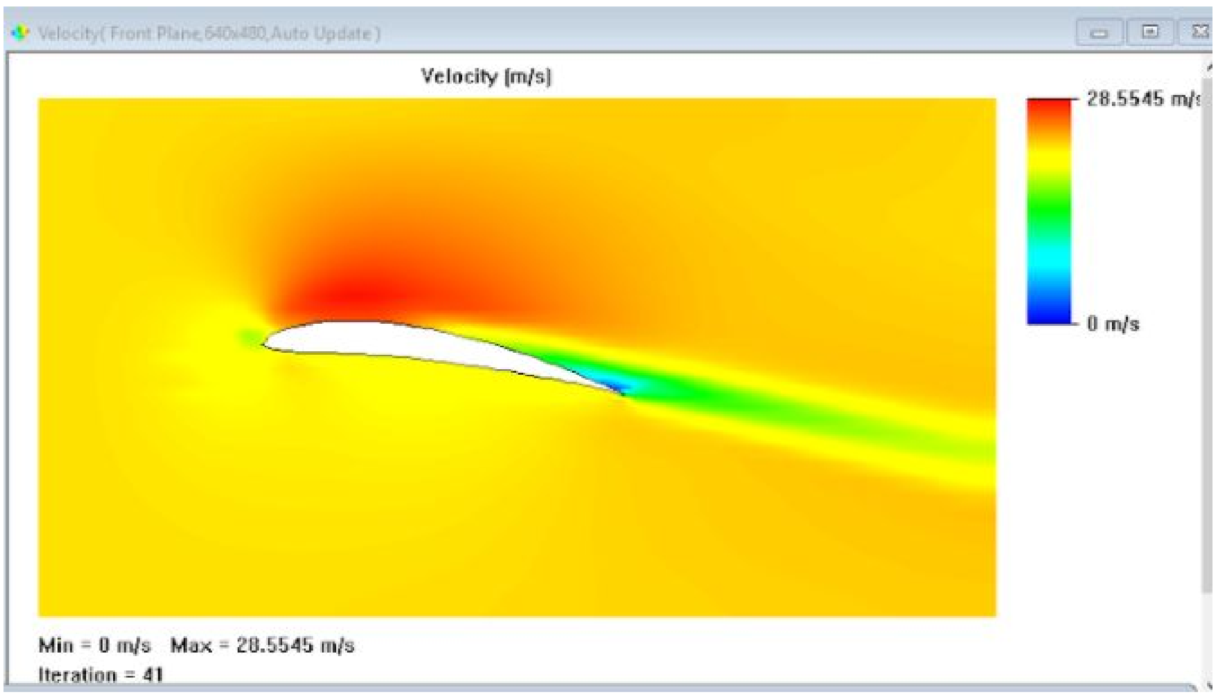

Figure 26. 2D Airfoil Profile Velocity Contour

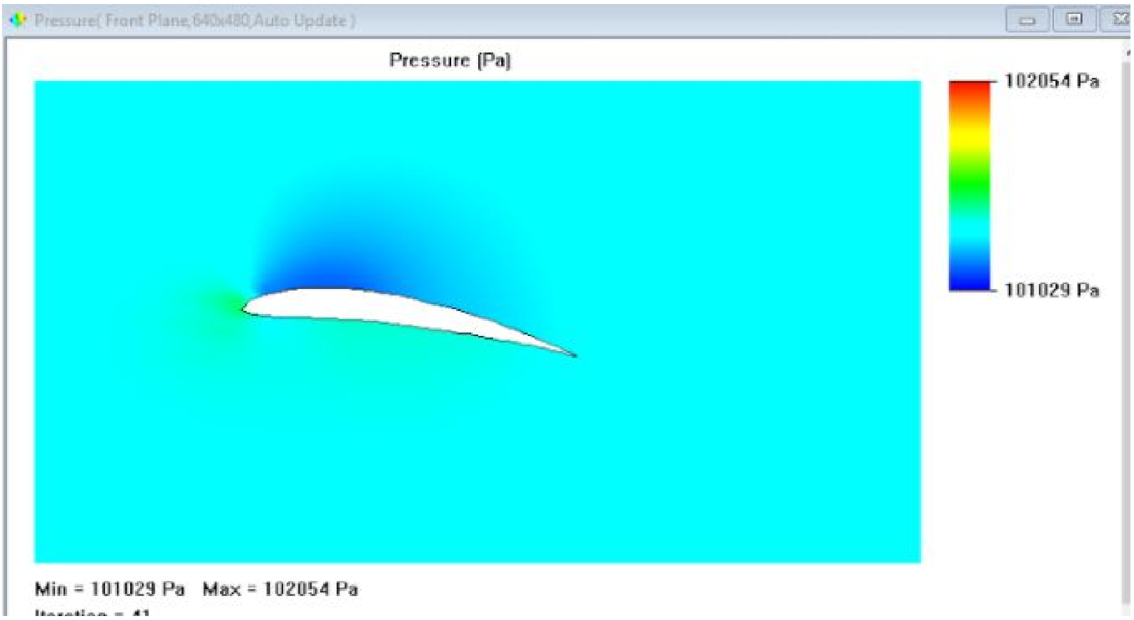

Figure 27. 2D Airfoil Profile Pressure Contour

M. Material Properties

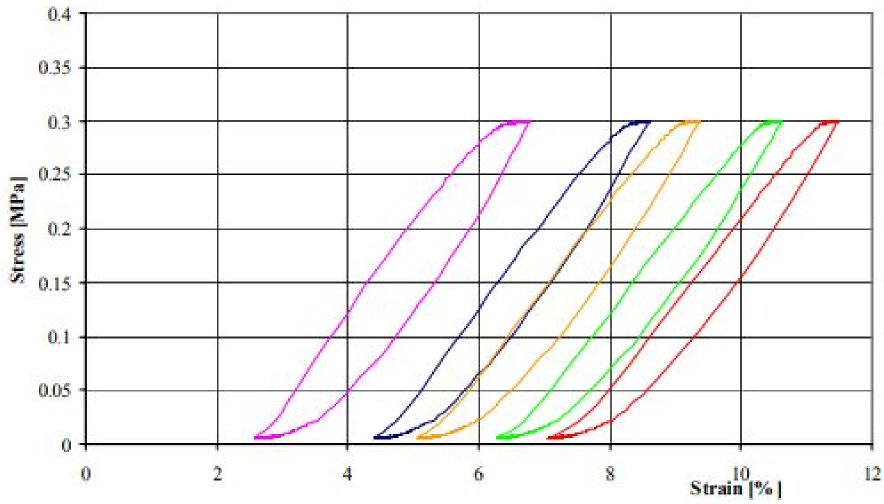

Figure 28. Rigid Polyurethane Foam Stress vs. Strain

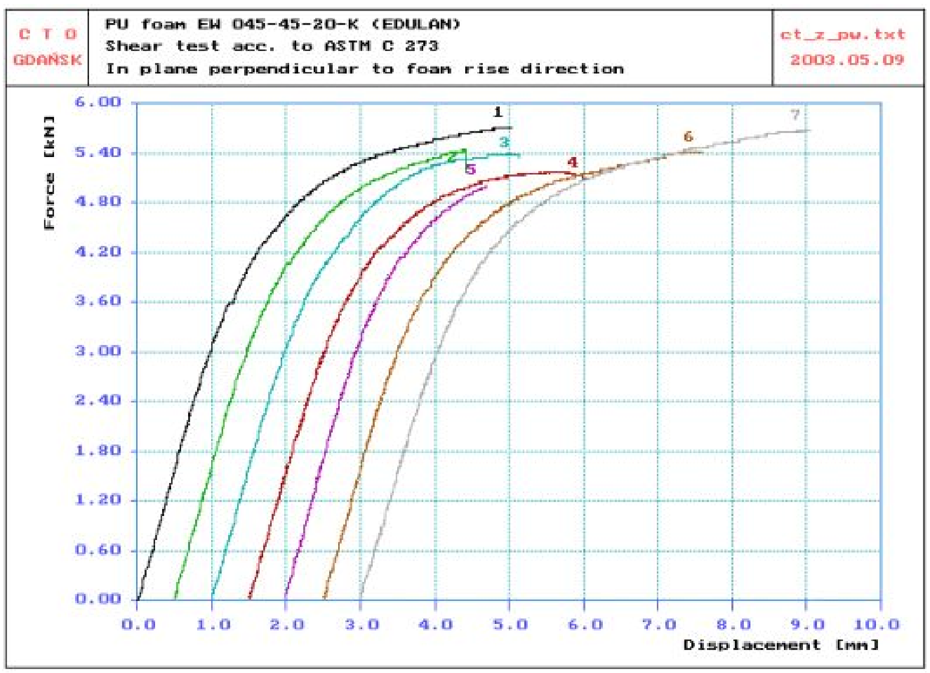

Figure 29. Rigid Polyurethane Foam Force vs Displacement

N. Horizontal Velocity

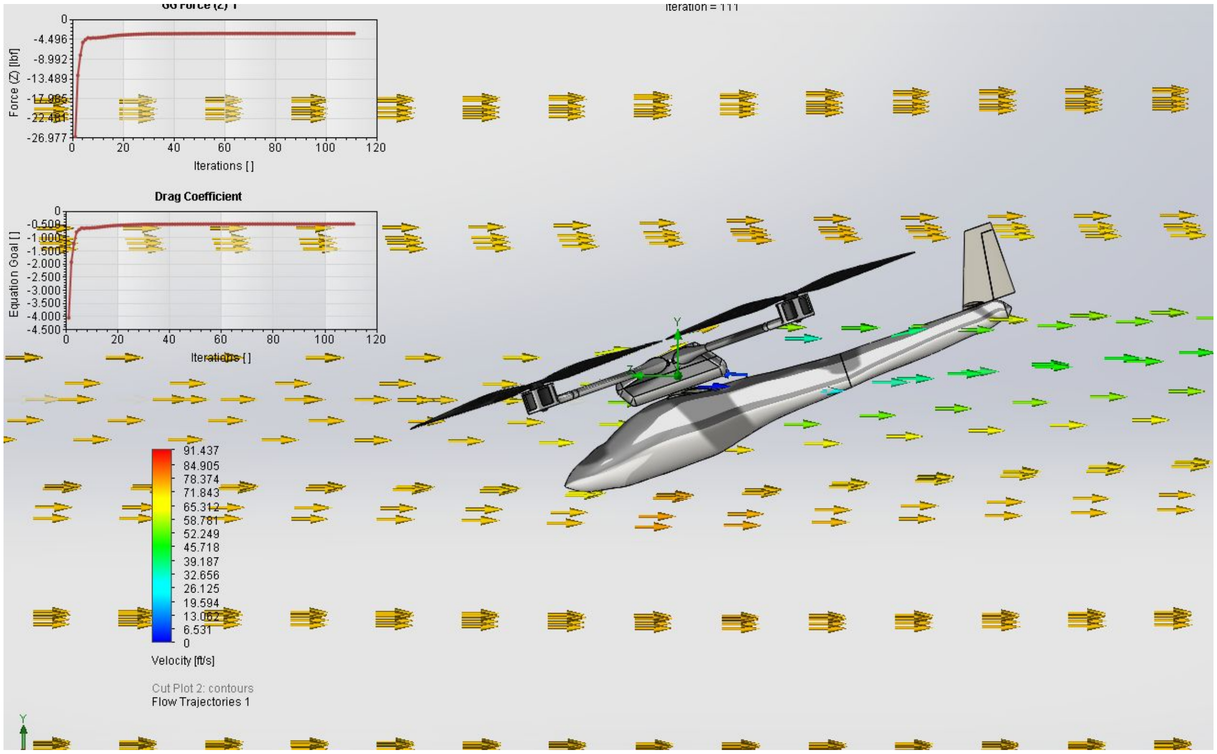

Figure 30. Pitched UAS Velocity Flow Trajectories

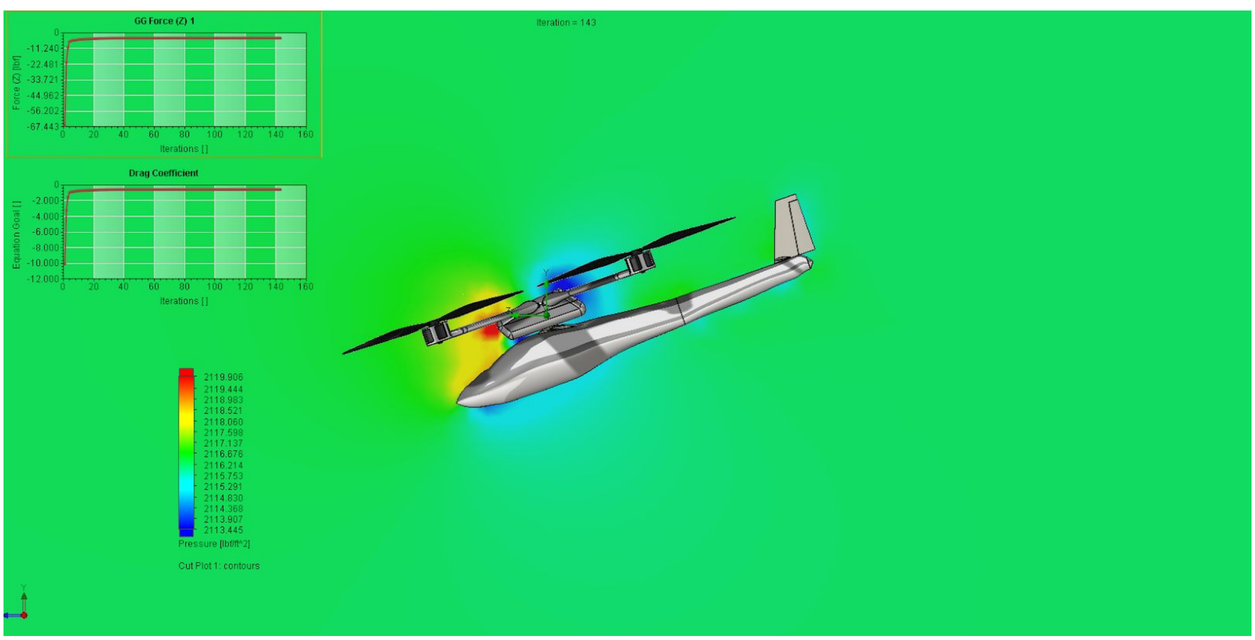

Figure 31. Pitched UAS Pressure Contour

Table 12. Pitched Propeller CFD Data

prop speed rear	Horizontal Force (lb)	Total Force (lb)	mesh	prop speed front	horizontal force	Total force (lb)	mesh	Total horizontal thrust force
735.13 rad/s	3.05	6.1	3	676.5 rad/s	2.613	5.226	3	22.6
	4.625	9.25	4		3.79855	7.5971	4	
	6.12	12.24	5		5.18	10.36	5	

Table 13. Total Quadcopter Distance Traveled vs. Velocity Data

Displacement Distance	Total Distance	velocity	Time min
2.497491902	4.994983804	113.2612578	2.646085998
2.756232092	5.512464183	105.129946	3.146085998
2.964948568	5.929897135	97.5824016	3.646085998
3.129490398	6.258980796	90.57671451	4.146085998
3.255124641	6.510249283	84.07398338	4.646085998
3.34658977	6.69317954	78.03809975	5.146085998
3.408144418	6.816288836	72.43554745	5.646085998
3.443611857	6.887223714	67.23521653	6.146085998
3.456420557	6.912841115	62.4082305	6.646085998
3.44964117	6.89928234	57.92778599	7.146085998
3.426020233	6.852040466	53.76900392	7.646085998
3.388010884	6.776021767	49.90879131	8.146085998
3.337800829	6.675601658	46.32571311	8.646085998
3.277337815	6.554675629	42.99987315	9.146085998
3.208352803	6.416705606	39.91280364	9.646085998
3.132381062	6.264762124	37.04736265	10.146086
3.050781342	6.101562685	34.38763891	10.646086
2.964753308	5.929506616	31.91886345	11.146086
2.875353378	5.750706755	29.62732762	11.646086
2.783509108	5.567018216	27.50030693	12.146086
2.690032252	5.380064503	25.52599043	12.646086
2.595630604	5.191261209	23.6934151	13.146086
2.500918748	5.001837495	21.99240498	13.646086
2.406427785	4.812855569	20.41351468	14.146086
2.312614159	4.625228318	18.9479769	14.646086
2.219867638	4.439735276	17.58765377	15.146086
2.128518532	4.257037063	16.32499168	15.646086
2.038844223	4.077688447	15.15297929	16.146086
1.951075066	3.902150132	14.06510864	16.646086

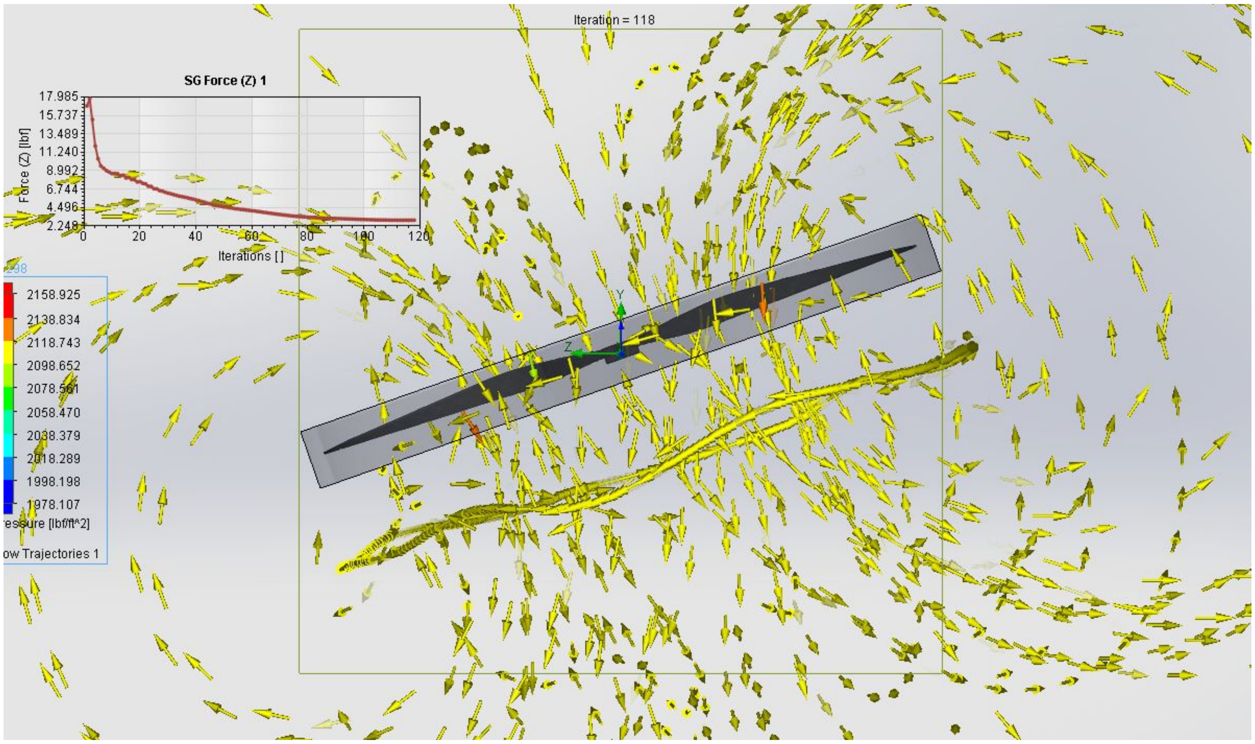

Figure 32. Pitched Propeller Pressure Flow Trajectories

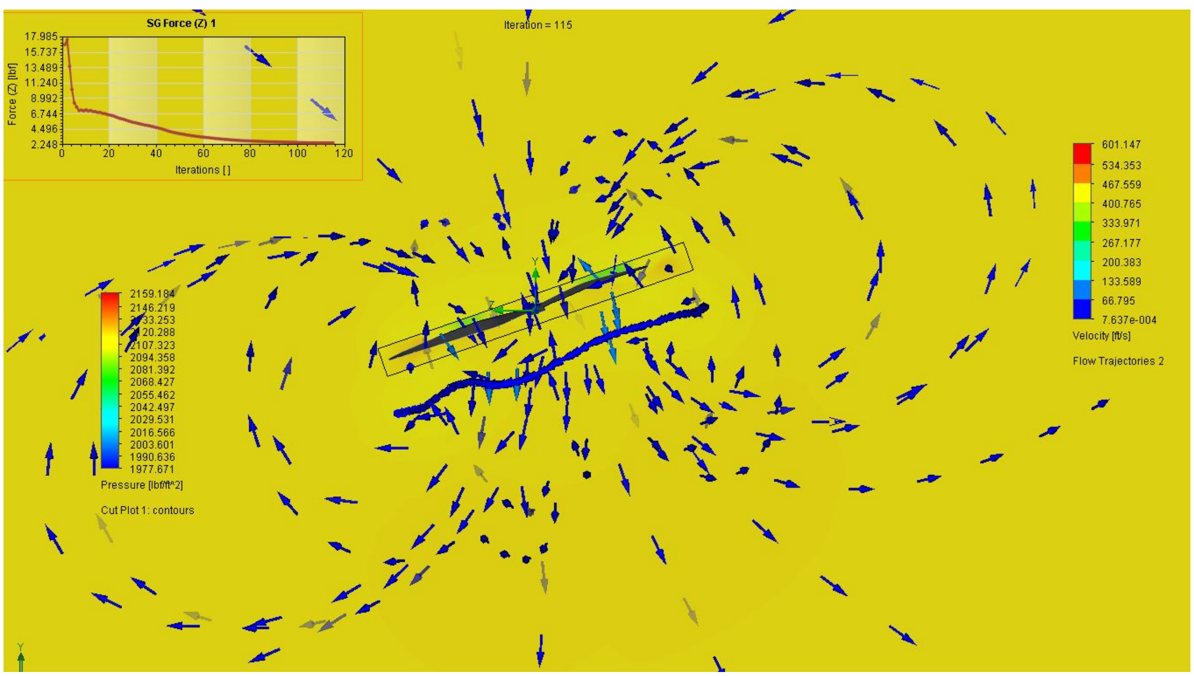

Figure 33. Pitched Propeller Velocity Flow Trajectories/Pressure Contours

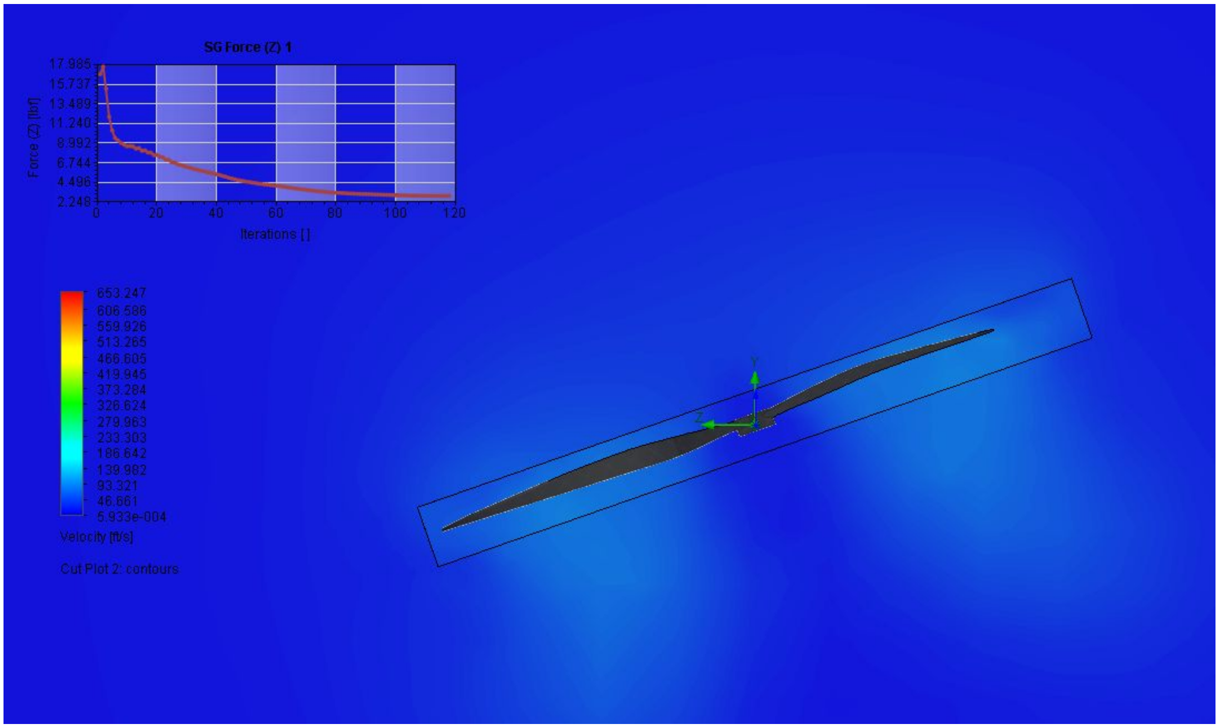

Figure 34. Pitched Propeller Velocity Contour

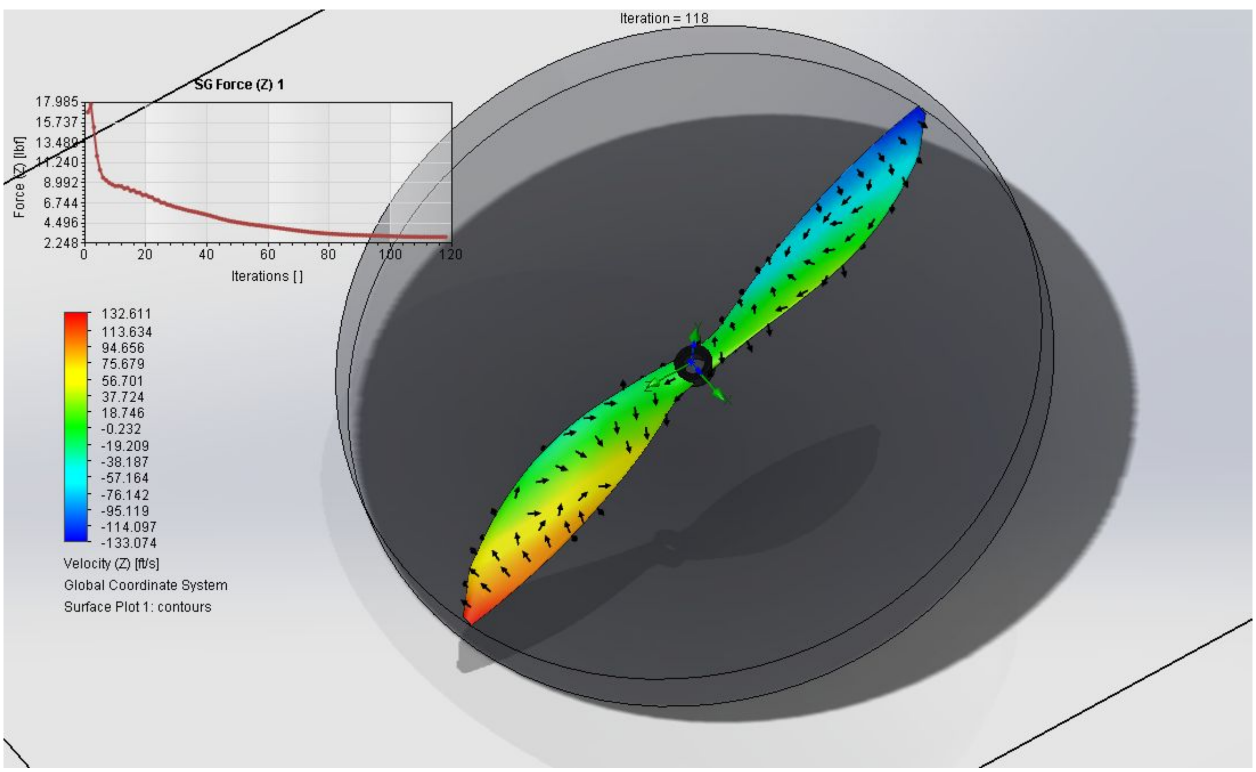

Figure 35. Pitched Propeller Velocity Surface Contours

Table 14. Horizontal Power Curve Data

			CFD	
Power Available (hp)	Velocity (fps)		Power Required (hp)	Velocity (fps)
0	0		0.011437568	22
0.2054545455	5		0.05218010321	36.67
0.4109090909	10		0.4593124545	73.33
0.6163636364	15		3.308311987	146.67
0.8218181818	20		6.474335616	183.33
1.027272727	25			
1.232727273	30			
1.438181818	35			
1.643636364	40			
1.849090909	45			
2.054545455	50			
2.26	55			
2.465454545	60			
2.670909091	65			
2.876363636	70			
3.081818182	75			
3.287272727	80			
3.492727273	85			
3.698181818	90			
3.903636364	95			
4.109090909	100			

O. Prototype

Figure 36. Working Model Components

Figure 37. Assembled Working Model Quadcopter

Figure 38. Assembled Working Model Quadcopter Rev-1

P. Assembled UAS Model

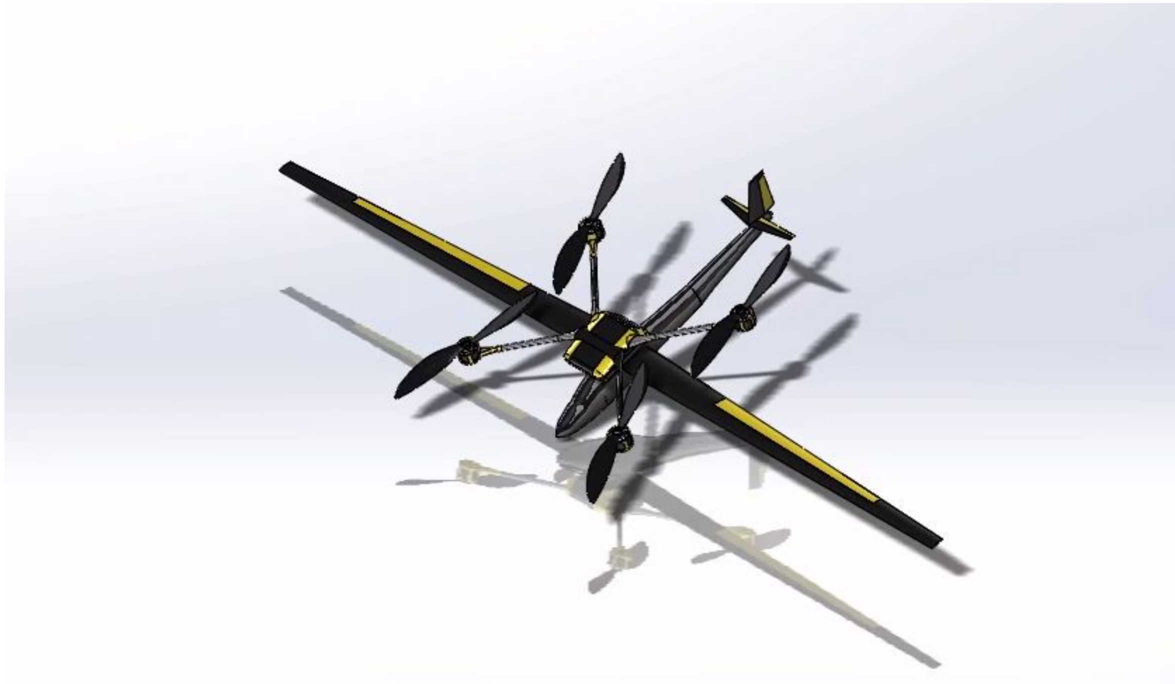

Figure 39. Assembled Conceptual UAS

Figure 40. Exploded Conceptual UAS

Q. UAS CAD Drawings

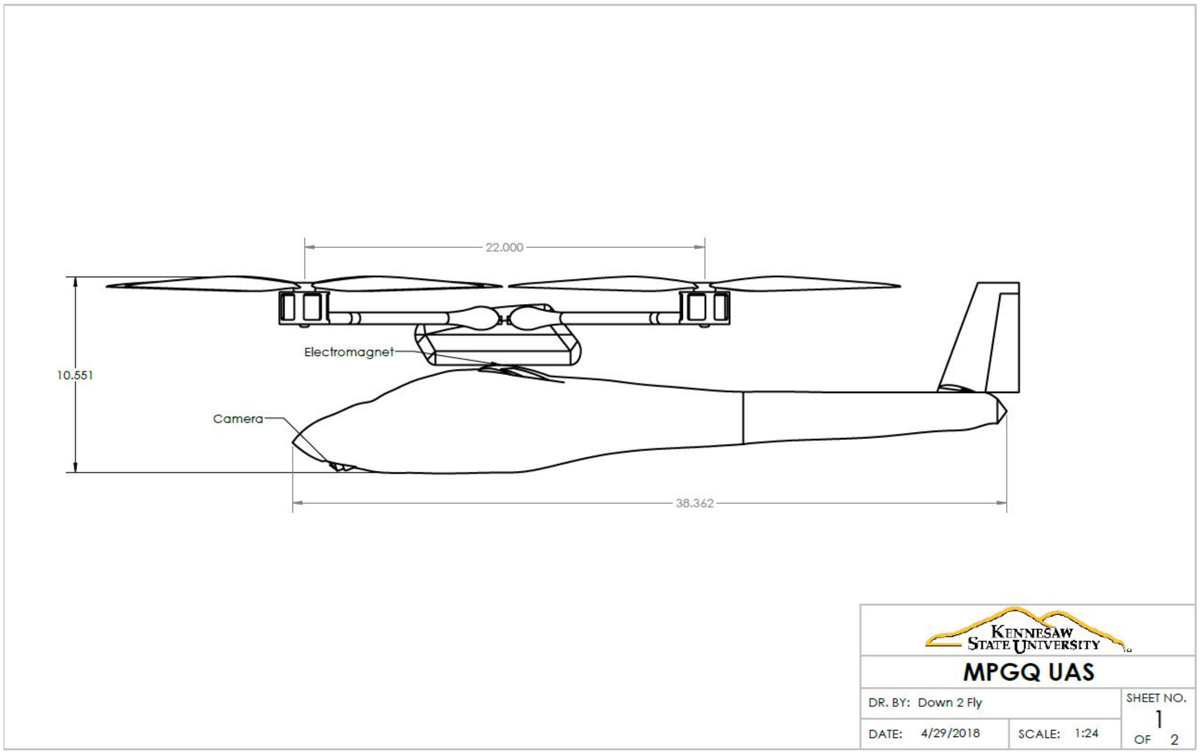

Figure 41. Right View UAS CAD Drawing

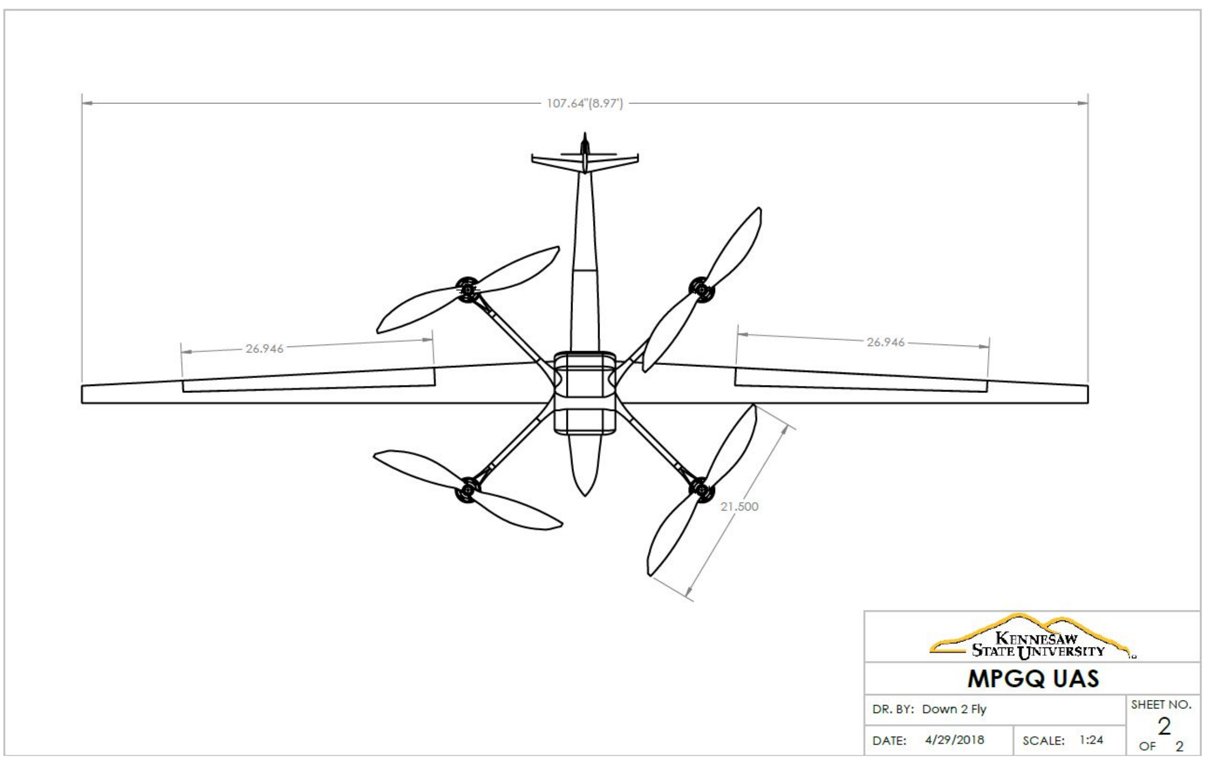

Figure 42. Top View UAS CAD Drawing